Converting Municipal Plastic Waste to Environmentally Friendly Fuel: A Process Simulation Study

by

Ankit Binekar

Submitted in partial fulfilment of the requirements
for the degree of Master of Applied Science

at

Dalhousie University
Halifax, Nova Scotia
August 2022

Table of Contents

List of Tables

List of Figures

Abstract

The amount of municipal plastic waste increases every year. Only 9% of the total plastic is recycled, but a substantial amount cannot be recycled, and most plastic goes to landfills. In this thesis, a process simulation model is implemented in the Aspen Plus® simulator, and the technical sensitivity analysis and optimization analysis are conducted for the distillation unit of a commercial pyrolysis plant.

The process simulation study was conducted for the actual plant capacity of 500 kg/hr of plastic waste under the temperature of 440°C and slight vacuum pressure of 0.998 atm to convert it into char, oil fuels, and non-condensable gases. Results show that the total oil fuel yield is 81.92% (heavy oil is 237.72 kg/hr and light oil is 171.90 kg/hr), whereas the non-condensable gases yield is 14.85%. The char yield is reduced to 3.22% due to the use of a secondary reactor that further pyrolyzes the char received from the primary reactors. The light oil and heavy oil fuel densities at 15°C are 759.36 kg/m^3 and 837.16 kg/m^3, similar to the density obtained from the fuel samples from the experimental runs.

A technical sensitivity analysis for liquid oils was performed across the columns RC-4601 and RC-4602 with two key variables: RC-4601 condenser duty and RC-4602 condenser duty. The maximum heavy oil production of 255.76 kg/hr can be achieved at RC-4601 condenser duty of -83.48 kW. However, the light oil production decreases to 159.83 kg/hr. At the critical point of -78.16 kW, the density of the heavy oil exceeds the standard density limit (850 kg/m^3). However, variations in RC-4601 condenser duty have shown no effect on the flash point of heavy oil. The optimum RC-4602 condenser duty obtained is -20.21 kW, where the light oil production rate is 182.07 kg/hr, increasing more than 5.91% over the predicted light oil production rate. At the critical point of -20.23 kW, the density of the light oil reduced to 756.17 kg/m^3. The flash point of light oil decreases with the increase in condenser cooling duty; a drop of more than 46% is observed from its maximum with the increase in condenser duty.

An optimization study predicted that the optimal range of condenser duty for RC-4601 is -78.21 to -78.16 kW and for RC-4602 is -23.84 to -23.85 kW. At the optimum condenser duty of -23.84 kW for RC-4602, the light oil production rate increases to 217.82 kg/hr, increasing more than 26.53% over the current operating production rate. The heavy oil production rate decreases at the condenser duty of -78.21 kW for RC-4601. However, with an increase in total condenser duty of 1.82%, the total production rate of oil fuels increases by 2.49% and the light oil to heavy oil production ratio increases from the current operating ratio of 0.72 to 1.08.

List of Abbreviations and Symbols Used

GC	Gas chromatography	
HDPE	High density polyethylene	
kWth	Kilowatt thermal capacity	
LDPE	Low density polyethylene	
M	Mass flowrate	kg/hr
min	Time in minute	
MS	Mass spectrometry	
MW	Molecular weight	
N_2	Nitrogen	
O_2	Oxygen	
P	Pressure	atm
PE	Polyethylene	
PET	Polyethylene Terephthalate	
PR	Peng Robinson	
PS	Polystyrene	
PP	Polypropylene	
PVC	Polyvinyl Chloride	
s	Time in seconds	
TGA	Thermo gravimetric analysis	
T	Temperature	°C
wt.%	Weight percentage	

Acknowledgements

I wish to thank all the people who have helped me during this work. First of all, I would like to thank and express my appreciation to my supervisor, Dr. Graham Gagnon, and administrative co-supervisor, Dr. Adam Donaldson, for guidance, freedom, and continued research support when needed.

I would sincerely like to thank Dr. Gianfranco Mazzanti, and Dr. Clifton Johnston, for sitting on the committee responsible for this thesis' review. And the support from the PEAS department: Ms. Julie O'Grady and Ms. Paula Colicchio.

I would like to gratefully acknowledge Mr. Peter Vinall for providing an opportunity to work with Sustane Technologies Inc. and thank him for providing valuable help and guidance and being supportive through this project. Special thanks also go to Mr. Keith Van Scotter for following the project and providing helpful advice. I wish to thank all the employees at Sustane who have helped me during this work. Everyone has been welcoming, helpful, and willing to share their knowledge. It has been a pleasant experience to be part of the team.

Finally, I would like to thank my family for always believing and supporting me. I am very fortunate to have two great families. Thank you Mr. Dhanraj Binekar, Mrs. Usha Binekar, Mr. David Rathbun, Mrs. Barbara Rathbun, Mrs. Kanchan Binekar-Wagh, Mrs. Shraddha Binekar-Kharikghare and Mrs. Pallavi Binekar-Katwe, for your constant support, encouragement, and unconditional love. I most definitely could not have done this without you.

1. Introduction

1.1. Need of Municipal Plastic Waste (MPW) Conversion into Fuel

Plastic has been a building block of improving the quality of everyday lives of modern human civilization. Plastics played a vital role in the innovation and development in various sectors such as packaging, automobile, construction, electronics, and healthcare. Rapidly growing industrialization and population increase have resulted in increased energy demands and rising municipal solid waste (biomass and plastic waste) across the globe. It is estimated that between 60 and 99 million metric tonnes of MPW were produced globally in 2015. This figure could triple to 155–265 million metric tonnes per year by 2060 if no actions are taken [1]. Also, Canada's commodity plastics demands are rapidly increasing and creating challenges in how to best manage municipal solid waste (MSW). Canadians produce 3 million tons of plastic waste every year; only 9% of total plastic waste is recycled with 2.7 million tons of plastics going to landfills or dumped into our natural environment [2].

Enormous amounts of waste plastics end up in the oceans, causing severe environmental and ecological problems. Globally, approximately 10–20 million tons of plastics end up in the oceans each year [3]. It is estimated that more than 5 trillion plastic pieces with a total weight of over 250,000 tonnes are currently floating in the oceans around the world [4]. The impact of this massive amount of plastic in the oceans, is projected to reach $13 billion in costs through ecological damages to marine habitats; financial damages to aquaculture, pisciculture, and

tourism, as well as remediation technologies implemented for cleaning polluted water bodies [3].

1.2. Current Situation in Nova Scotia

Similarly, Nova Scotia is currently experiencing challenges with escalating MSW. The population of Nova Scotia is over 0.9 million, and waste per person entering dumps is 380 kilograms, which is far from achieving the reduction goal of 300 kilograms per person [5].

The municipalities in Nova Scotia are now spending $25 million a year on recycling MSW, which represents a substantial increase of 56% over the last decade. Nova Scotia has 63 publicly owned waste management facilities and most of the landfills in the province are very small and considered inefficient. The total cost of waste management is projected to increase from $140 million to more than $200 million by 2040 if no significant measures are taken [5]. Municipal plastic waste (MPW) accounts for 21% of total municipal solid waste, which creates significant savings opportunities if MPW can be diverted from landfills.

1.3. Municipal Plastic Waste and Need for Plastic Pyrolysis

In order to reduce plastic waste disposal to the landfill, recycling methods are considered essential to manage MPW. There are four main categories of recycling methods, namely primary recycling (re-extrusion recycling), secondary recycling (mechanical recycling), tertiary recycling (chemical recycling), as well as quaternary recycling (energy recovery) [6].

As noted earlier, only 9% of total plastic waste is recycled. Recycling efforts utilize primary and secondary recycling methods, which have proven to be very difficult and cost-ineffective because these methods require homogenous and contaminant-free feedstock.

Chemical recycling methods, such as pyrolysis, involves thermal energy and chemical agents to change the polymeric structure of the final product. This method can help reconcile the tremendous pressure to reduce the use of fossil fuels with increasing demand for plastics. Therefore, the chemical recycling method has proven to be the most reliable and sustainable because its final product is the raw material from which the plastics are made initially.

The quaternary recycling method is an energy recovery method where plastic waste is used to generate heat and electricity through combustion and is not environmentally friendly due to resulting pollutants.

The chemical recycling method is gaining far more attention than the quaternary recycling method as it can recover the energy content of the plastic waste in the form of liquid and gas, which is easy to store and transport. Of the chemical recycling methods plastic pyrolysis is the most flexible and efficient.

1.4. Environmental Impact

Plastic pyrolysis technology conserves land resources and lowers waste management capital expenditures by reducing the plastics inflow to landfills and oceans. This technology has high conversion efficiency and cost-effectiveness and generates employment by utilizing waste plastics to produce valuable energy. This

could be an alternative energy resource for fossil fuels such as diesel, which have severe contaminants such as sulphur.

Sulphur content in the fuel is one of the significant parameters used to analyze the fuel quality because sulphur content could form SO_2 after combustion. SO_2 is a pollutant causing severe air pollution, affecting people's health, and damaging concrete structures. In 2019, there were 6 (out of 14) refiners at or below the 10 ppm in Canada; 5 refiners had sulphur content higher than 10 ppm, but below 20 ppm, and 3 had sulphur content closer to 30 ppm [7].

1.5. Economically Viability and Sustainability

Plastic is a valuable material and resource because of its high functionality, durability, and low cost. In Canada, plastic production is a $35 billion industry employing approximately 100,000 people in nearly 2,000 businesses. The Government of Canada plans to achieve zero plastic waste by 2030. The zero plastic waste visions require plastic to stay in the economy and out of landfills and the environment with an aim to develop a plastic circular economy [8]. In plastic, carbon and hydrogen make up the majority (more than 90%) of the total content, and therefore, most plastics have high volatile content. Reusing this volatile matter contributes towards the plastic circular economy.

Environment and Climate Change Canada has invested about $2 million in the zero-plastic waste initiative. This fund will support new projects to implement innovative community solutions across Canada. The recent projection claims these new projects will lead to a measurable reduction of pollution caused by

plastic waste in Canada and support the development of a new plastic circular economy. Developing a sustainable plastic circular economy is projected to reduce 1.8 million tonnes of greenhouse gas emissions per year and create approximately 42,000 jobs across Canada [8].

1.6. Thesis Objectives

The overall objective of this thesis is to develop an effective process simulation model for the plastic pyrolysis process of Sustane Technology Inc. that can be used to analyze and then optimize the distillation unit of their pyrolysis process.

The first phase of the thesis is the development of an effective process simulation model using Aspen Plus® software that would replicate the crucial parameters such as temperature, pressure and flowrate of process streams and physical properties such as viscosity, density, and flash point of oil fuels from the Sustane plant in Chester, NS. The developed process simulation model is used to evaluate the production of light oil and heavy oil fuel.

The second phase of the thesis utilizes the simulation process model to optimize the distillation unit, mainly focusing on the production yield of light oil and heavy oil through a technical sensitivity analysis and an optimization analysis. There was a particular emphasis on light oil due to its high economic value as it requires less processing for petrochemical companies to use in the production of plastic and other chemicals.

1.7. Thesis Structure

This thesis is divided into seven sections. Section 1, Introduction. Section 2 discusses literature available on the plastic pyrolysis process and other experimental results that have been achieved.

Section 3 summaries are provided for relevant and important studies for the simulation plastic pyrolysis process. Significant findings, advantages, and disadvantages of these studies and their significance are briefly discussed.

Section 4 describes the plastic pyrolysis process of Sustane. Their process design, process parameters, and process flow diagram are included. The procedure for collecting process parameters and equipment design data is provided. A detailed discussion describes the characterization of the data collected from the lab analysis of the samples used in the simulation.

Section 5 provides an approach and a description of the model development. It also highlights the development of the model in Aspen Plus® version 10, including template settings and thermodynamic property method, i.e., equation of state, fundamental equipment modules, and assumptions. It provides an overview of the Aspen Plus® model layout and discusses the simulation configuration and the parameters used in the simulation.

Section 6 outlines the results and discusses the work, starting with a material and energy balance from the study. Results from the Aspen Plus® model are then analyzed and compared with the lab sample data. Finally, the sensitivity analysis and the optimization analysis results are provided.

Section 7 summarizes the conclusion of the study, reviews significant findings, troubleshooting, and highlights post-analysis recommendations. These recommendations will be used for further optimization of the existing plant.

2. Introduction to Plastic Pyrolysis Process

In an effort to recycle plastic waste, many processes have been developed over the years. As noted in section 1.3, chemical recycling processes are gaining more attention. In the chemical recycling process, MPW is depolymerized into monomers or other chemicals using thermal energy and chemical agents. It requires less sorting and is highly efficient and inexpensive compared to other recycling processes.

2.1. Methods for Converting Plastic to Environmentally Friendly Fuel

Chemical processes that convert plastic waste into environmentally friendly fuels have been developed and are broadly divided into three categories; Hydrocracking, Gasification, and Pyrolysis [9].

2.1.1. Hydrocracking

Hydrocracking is the process in which the heavy long-chain hydrocarbon polymers are depolymerized into lighter small molecules by adding hydrogen under high temperature and pressure in the presence of a catalyst [10]. It is also called hydrogenation. The sole thermal heating of plastics such as PS releases aromatic compounds such as benzene and xylene because of the styrene structure of the plastic, which decreases the quality of the fuel. In the hydrocracking process, hydrogen reduces aromatic compounds to small-chain saturated hydrocarbon compounds. The usage of excess hydrogen eliminates heteroatoms such as chlorine, bromine, and fluorine present in plastic [6]. Therefore, hydrocracking can

convert waste plastics into high-quality liquid fuels and provide highly saturated liquid fuel products [11].

Also, the hydrocracking process requires expensive high operating pressure equipment because it operates under the pressure range of 19.7-148 atm [9].

2.1.2. Gasification

Gasification is the combustion process that converts plastic waste mainly into synthesis gas, also known as syngas (i.e., CO, CO_2, H_2) in the presence of oxygen and steam at 1200-1500°C [12]. The syngas contains undesired products such as particulate matter, alkali metals and sulphides, tar etc. The syngas obtained during the gasification process is converted into liquid fuels by the following processes:

2.1.2.1. Fischer-Tropsch Synthesis

Fischer-Tropsch (FT) synthesis is the chemical catalytic process that converts syngas derived from coal, biomass, and natural gas into liquid fuels. FT process operates at the high pressure of 20-50 atm. Iron and cobalt-based catalyst are used, which affect the operating temperature of the process. The FT process can be operated over a wide range of temperatures 220–350°C for iron-based catalyst and 200–240°C for cobalt-based catalyst [13].

Although the FT process is known for converting syngas to liquid fuels, it has various disadvantages. FT is very energy and capital-intensive process. In addition, the FT process is sensitive to contaminants such as sulphur and requires a specific H_2/CO ratio for better efficiency of product yield [14]. Also, it provides less selectivity of desired products [15].

2.1.2.2. Syngas Fermentation (Bioconversion)

Syngas fermentation is the biological method to produce biofuels such as acetic acid, ethanol, butanol, etc., by using anaerobic microbial fermentation. Various microorganisms such as Clostridium Ragsdale, Butyribacterium methylotrophicum, Clostridium carboxidivorans P7, Clostridium ljungdahli, and Clostridium auto-ethanogenum, etc. are used in syngas fermentation that follows the Wood Ljungdahl pathway (also called the acetyl-CoA pathway) to convert syngas into products such as acetate and then alcohols [14]. The production of acetic acid and ethanol from syngas follows a series of sequences set of elementary chemical reactions, and each reaction proceeds with an associated enzyme within a cell. Enzymes mediate reactions inside the cell, and each enzyme compels a specific reactant and converts them into particular products. These enzymatic reactions are typically reversible [16]. Usually, this process was carried out at low pressures (1 to 2 atm) and low temperatures (25 to 37°C). The pH of the process is an essential factor that depends on the type of microorganism used in the process.

Although the syngas fermentation process requires less energy, this process is challenging to scale commercially because of the low mass transfer rate of the gaseous substrate into the liquid culture medium. This is due to the low aqueous solubility of the sparingly soluble gaseous substrates such as CO and H_2. On a molar basis at 35^{o}C, the solubility of CO and H_2 are 77% and 68%, respectively, to that of oxygen [17]. Because of this diffusion limitation, the availability of gaseous substrate for the microorganism becomes low, ultimately reducing process productivity.

FT synthesis and syngas fermentation are two-stage processes; the plastic is first gasified into syngas (CO, CO_2 and H_2), and then syngas is converted into fuels.

2.1.3. Pyrolysis

Pyrolysis is the thermal degradation of long-chain polymer molecules such as plastic waste in the absence of oxygen to produce gas, liquid, and solid products. Thermal degradation involves cracking large chain hydrocarbon such as plastic into small chain hydrocarbons at different high temperatures (300–900°C) [18]. The pyrolysis process does not cause water contamination like plastic recycling.

Pyrolysis is an endothermic process. In this process, the waste plastics are crushed into small pieces and heated directly, improving the heat transfer profile and producing value-added products. Also, it is considered a green technology. It is one of the gaseous products with a substantial calorific value that can be reused to compensate for the overall energy requirement of the pyrolysis plant [19]. The liquid products of plastic pyrolysis consist of both gasoline and diesel range hydrocarbon [20]. The remaining output of the process is solid pyro-char that could be easily used as a road laying or a feedstock for other applications [21].

2.1.3.1. Advantages of pyrolysis process

Of the three categories of the chemical process, Hydrocracking and Gasification have significant constraints for successful commercialization whereas Pyrolysis has the greatest potential for successful commercialization.

The Hydrocracking process has high capital requirements and high operating costs. Similarly, both Gasification processes have high capital requirements and/or high operating costs and scalability constraints.

In contrast, the pyrolysis process is the most commercialized process due to its low cost of production and operation, uncomplicated and flexible process [22].

The three major products produced during pyrolysis are oil, gas, and char, valuable for industries, mainly petrochemical and refineries. In addition, pyrolysis is also very flexible since the process parameters can be manipulated to optimize the product yield based on preferences. The process handling is also much more straightforward and flexible than the other processes.

2.2. Fundamental Aspects of Plastic Pyrolysis

A simplified general pyrolysis process overview is presented in Fig. 2.1.

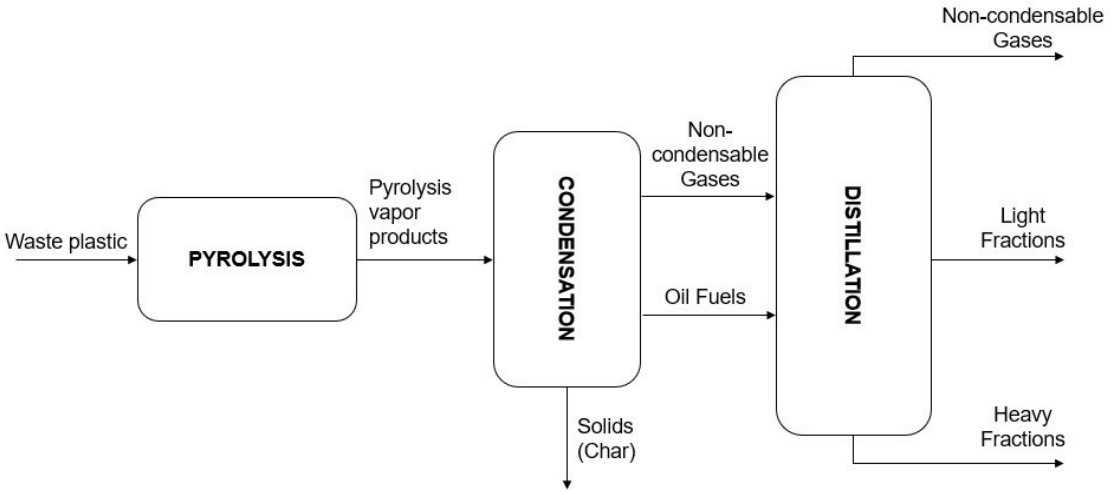

Fig. 2.1: General overview of pyrolysis process.

As shown in Fig. 2.1, waste-plastic comes in the pyrolysis cracking unit where three products, gas, oil, and char (solids), are yielded. The overall terminology of the pyrolysis process is explained in reaction 1.

Plastic polymer + Heat $\longrightarrow$ Gas + Liquid + Char (1)

The oil typically has a broad composition and is fractionated in the distillation unit. The actual design of the units and process parameters may differ widely, depending on feed composition, environment, and the kind of products desired concerning the demand in the market.

It is essential to know its mechanism to understand the pyrolysis process and control it. In plastic pyrolysis, high temperature is the most critical cause of breaking the hydrocarbon chain. The carbon-carbon and carbon-hydrogen bond demand high activation energy in an inert atmosphere without oxygen [20].

The pyrolysis process of plastic is a typical radical chain mechanism, where initiation, propagation (transfer and decomposition), and termination reactions occur. This reaction mechanism is explained in detail by T. Faravelli et al. [23]. The decomposition mechanism of different plastic polymers and their monomer yields are given in Table 2.1.

Table 2.1: Polymer decomposition mechanisms and percentage yield of monomer [24].

Plastic polymers	Decomposition mechanisms	Yield of monomer (weight %)
Polyethylene terephthalate (PET)	End-chain scission	95
Polyethylene (PE)	Random-chain scission	0.03
Polyvinyl chloride (PVC)	Chain-stripping	0-0.07
Polypropylene (PP)	Random-chain scission	0–17
Polystyrene (PS)	End-chain and random-chain scission	42–45

2.3. Factors Affecting the Plastic Pyrolysis Process

The critical factors affecting the pyrolysis process and its product range and distribution include the chemical composition of the feedstock, the type of reactor used, reactor temperature, residence time, and reactor pressure. These factors are explained briefly in the following section.

2.3.1. Chemical Composition of Feedstock

Plastics can be categorized according to the chemical structure of polymer molecules such as linear, branched, or cross-linked is shown in Fig. 2.2.

Linear 

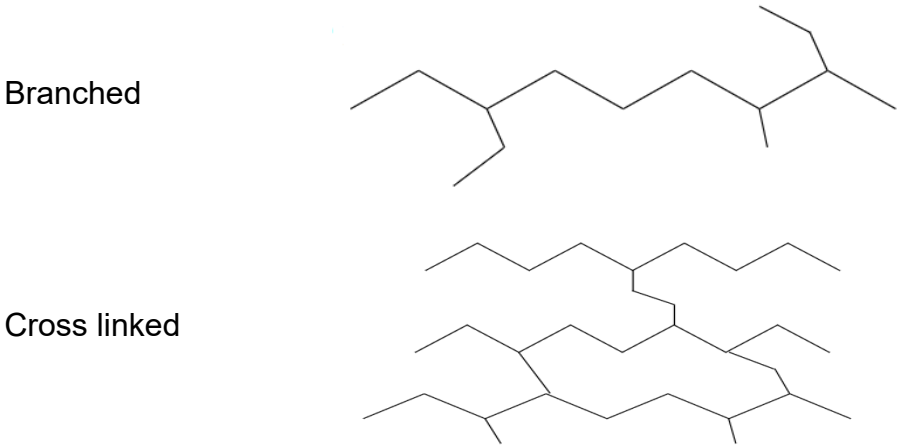

Fig. 2.2: Examples of different polymer structures of plastic found in MSW

The groups are connected only to two other groups in linear polymers, one to each end. Whereas in branched polymers, at least one of the monomers group is connected to more than two functional groups. It has been found that there is a significant inverse relationship between the polymer density and its branching intensity. More branched polymers have relatively lower densities. Therefore, the linear PE is called high-density polyethylene (HDPE), and the branched PE is called low-density polyethylene (LDPE). A cross-linked polymer is an interconnected branched polymer with all polymer chains to form a large molecule.

Different plastics have different compositions and chemical properties dependent upon four particular components: moisture content, fixed carbon, volatile matter, and ash content [19]. The pyrolysis products are directly dependent on the chemical composition and these components of the plastics to be pyrolyzed. High volatile matter is solely responsible for liquid oil production, whereas high ash content decreases the amount of liquid oil, subsequently increasing the gaseous

yield and char formation [25]. The chemical composition of the overall mixed plastic feedstock also affects the pyrolysis process.

The summary of the chemical contents of different plastic is given in Table 2.2 and shows that all plastics have high volatile matter and low ash content. The data indicates a high potential to produce liquid oil from pyrolyzing plastic waste.

Table 2.2: Chemical content of plastics [20,25].

Type of plastics	Moisture (wt.%)	Fixed carbon (wt.%)	Volatile (wt.%)	Ash (wt.%)
PET	0.46 - 0.61	7.77 - 13.17	86.83 - 91.75	0.00 - 0.02
HDPE	0.00	0.01 - 0.03	98.57 - 99.81	0.18 - 1.40
PVC	0.74 - 0.80	5.19 - 6.30	93.70 - 94.82	0.00
LDPE	0.3	-	99.60 - 99.70	0.00 - 0.40
PP	0.15 - 0.18	0.16 - 1.22	95.08 - 97.85	1.99 - 3.55
PS	0.25 - 0.3	0.12 - 0.20	99.50 - 99.63	0.00
Others	0.00 - 0.16	0.04 - 2.88	97.12 - 98.87	0.00 – 1.01

Pyrolizing the plastic wastes produces various hydrocarbon products such as paraffin, olefins, and aromatics. But the quality of the hydrocarbon products is determined by the volatility [24].

Volatility is an important factor that determines the quality of the hydrocarbon product. Light hydrocarbons have higher volatilities, and heavy hydrocarbons have low volatilities. Lighter hydrocarbons are easier to crack for chemical recycling

through thermal cracking and catalytic cracking. Also, good volatile hydrocarbon products can be used as petrol and diesel in combustion engines.

At Sustane, plastic waste goes through a series of mechanical separation processes. Plastics such as PVC, PTFE and PET are removed and not pyrolyzed because of chlorine, fluorine and oxygen atoms. They form a chlorinated, fluorinated and oxygenated compound harmful to human health and the environment.

2.3.2. Type of Reactor

In the pyrolysis process, the type of reactors plays the most important role in product formation. It significantly influences the mixing of the plastics with pyrolysis products and catalysts, reactor residence time, heat transfer rate, and reaction efficiency towards achieving the final desired product. Reactors are classified into batch and semi-batch, fixed and fluidized bed reactor, conical spouted bed reactor and, microwave reactor. The operation, advantages, and disadvantages of the various reactor types are discussed in detail as follows:

2.3.2.1. Batch and Semi-batch Reactor

Batch and semi-batch reactors are widely used reactors in the pyrolysis process. Both the reactors are mainly used for research purposes. There is no flow of the reactant or product in the batch reactor while the pyrolysis reaction is being carried out. The semi-batch reactor allows pyrolysis product removal and reactant feed addition in time. The batch reactor is said to have the advantage of enabling the reactant in the reactor for an extended period of time, thus providing high

conversion. Similarly, the flexibility that a semi-batch reactor offers to add reactants over a period of time offers better reaction selectivity. However, some disadvantages of these reactors include variability of products, high labour costs, and the difficulty of scaling to large production [19].

Another study was conducted by Miandad et al. [26] to examine the effect of different plastic waste types such as PP, PE, PS, and PET on the yield and quality of produced liquid oil from the pyrolysis process using a batch reactor. The pyrolysis was conducted at 450°C with a residence time of 75 min. It was reported that as compared to the other plastics, PS pyrolysis resulted in the maximum liquid oil yield of 80.8%, along with the lowest gas and char yield of 13 wt.% and 6.2 wt.%, respectively. Whereas pyrolysis of PE reported the lowest liquid oil yield and pyrolysis of PS/PE (50/50) mixture reported highest gases yield of 69.9% and liquid oil yield of 25%. Also, it has been found liquid oil from all types of plastic consists of mostly aromatic compounds with some alkanes and alkenes. Abbas-Abadi et al. [27] reported a very high liquid yield of 92.3 wt.% from the PP pyrolysis experiment. This study used an FCC catalyst at 450°C in a semi-batch reactor.

2.3.2.2. Fixed and Fluidized Bed Reactor

The pyrolysis reactor can be classified into fixed and fluidized bed reactors depending on the heat transfer method and flow pattern the feed and products. In the fixed bed reactor, the catalysts are packed in a stationary bed, which is a simple design and easy to operate. However, there are some constraints with fixed bed reactors, such as the irregular sizes and shapes of the plastics feedstock, that may cause problems during the feeding process in a continuous process [19]. Also,

there is a large temperature gradient caused by the low thermal conductivity of the plastic feed.

In most studies, fixed bed reactors are used as secondary reactors in a two-step reactor system. This is because the products from the primary pyrolysis reactor are mainly gaseous and liquid phase, thus offering better gas-liquid contact in the fixed bed reactor. Vasile et al. [28], Uemichi et al. [29], and Onu et al. [30] have used a catalytic fixed bed reactor as a second reactor in the two-step plastics pyrolysis experiments.

Fluidized bed reactors are among the most widely used reactors for the pyrolysis process as it overcomes some of the issues while using a fixed bed reactor [19]. The main advantages that a fluidized bed reactor offers are the homogeneity of temperature and composition. Plastic polymers have very low thermal conductivity and high viscosity. Because of this, heat is not properly transferred (poor thermal conductivity) for the cracking of polymers during the plastic pyrolysis process. A fluidized bed offers better thermal conductivity than a fixed bed and other reactors, which provide high heat and mass transfer rates. One of the critical parameters that affect the pyrolysis process and its product distribution is the catalyst bed's dimension and material [31]. The fluidized bed catalyst offers a huge surface area for the reaction to occur since it is in the fluid state and well mixed.

Many researchers have preferred fluidized bed reactor in the plastic pyrolysis process. In the most extensive study, Kaminsky et al. [32] chose to use the Hamburg process, using an indirectly heated fluidized bed reactor for pyrolysis of PP, PE, PP, PS, PVC, the mixture of different plastics, and many others. In this

thermal pyrolysis process, the fluidized bed reactors were operated at a temperature from 450°C to 787°C. The author reported that PE produced a high liquid oil yield of 50.3 wt.% in addition to 42 wt.% wax at 530°C while 42.4 wt.% of liquid oil yield at 760°C. He has also reported a low char yield of 0.1 wt.% and 0.18 wt.%, respectively. The highest yield is reported for PS with the total liquid oil yield of 89.5 wt.%, including 64.9 wt.% of pure styrene at 580 wt.%. Williams et al. [33] conducted an LDPE pyrolysis study using a fluidized bed reactor to illustrate the influence of pyrolysis temperature from 500°C to 700°C on the yield and composition of derived products. It is reported that LDPE produced a high liquid oil yield of 89.2 wt.% at 500°C and the lowest gas yield of 10.8 wt.%. The liquid oil yield decreased from 75.8 wt.% to 28.6 wt.% with an increase in temperature from 600°C to 700°C, respectively.

Conversely, there was a steep increase in gas yield of 24.2 wt.% to 71.4 wt.% with an increased pyrolysis temperature from 600°C to 700°C, respectively. The author further concluded based on the analysis of derived oils and waxes that the decrease in liquid oil yield with the increase in pyrolysis temperature is because the pyrolysis of LDPE gave a mainly aliphatic composition consisting of a series of alkanes, alkenes, and alkadienes. The liquid oil appeared to increase aromatic composition with increasing pyrolysis temperature and identified a significant concentration of single ring and polycyclic aromatic hydrocarbon compounds at 700°C.

It is clear from the literature that fluidized bed reactors can be used for the thermal and catalytic plastic pyrolysis process. It is more flexible than the batch reactor as

regular feedstock charging and can eliminate catalyst reuse problems. It can claim that the fluidized bed reactor is more suitable for industrial-scale operation.

2.3.2.3. Rotary Kiln Reactor

A new reactor system known as a rotary kiln reactor has recently emerged and has been widely used in the plastic pyrolysis industry. It is considered more efficient than the fixed-bed reactor because it can quickly heat the feedstock and provide a desirable heating profile. The rotary kiln reactors are externally heated using fuel or electricity, and the use of a slowly rotating inclined kiln provides a good blending of the feedstock that undergoes thermal degradation with the formation of char, liquid, and gas products in the desired proportions. Compared to a fixed bed reactor, the rotary kiln reactor has the advantage of the ease of operation and maintenance and uses a simple plastic feeding process. It also provides a high degree of flexibility in adjusting the residence time and heating rates.

Many clean technology companies have used rotary kiln reactor systems for pyrolysis technologies. Switzerland's Ticino Canton waste treatment center used PYROPLEQ® technology for the plastic pyrolysis process that employs a rotary kiln reactor system. They successfully ran this pyrolysis process at 500°C and produced the char with a high calorific value [34].

Similarly, many researchers have preferred a rotary kiln reactor in the plastic pyrolysis process. Recently, Zhang et al. [35] conducted a waste plastic pyrolysis experiment using a rotary kiln reactor to recover liquid oil and study the effect of

heat carrier filling ratio (a ratio of heat carrier bed volume to reactor volume) and the type of plastic waste on the product spectrum and quality. They found that the optimized heat carrier filling ratio is 15% for oil production. They also reported that mixed plastic waste yields a high liquid oil yield of 89.5% with a wide gasoline hydrocarbon range.

2.3.2.4. Microwave-Assisted Technology

With the commercialization of the plastic pyrolysis process, new technologies are emerging to develop plastic pyrolysis. One such technology that has become very attractive in recent years is Microwave-assisted technology. Microwave-assisted technology uses electromagnetic waves to heat materials through dielectric heating. In general, plastic polymers do not have strong dielectric properties, making them insensitive to this technology. Therefore, highly microwave-absorbent material such a particulate carbon is added with the plastic waste to make heating efficient. There have been few experiments dedicated to studying the different structures of carbon and other carbonaceous material as microwave-absorbent. These microwave absorbents absorb microwave energy that generates enough thermal energy to start the thermal degradation of plastic polymers. Since this technology is relatively new, it is challenging to report the advantages and disadvantages over conventional methods.

Few studies have been done on plastic pyrolysis using microwave-assisted reactors. Russel et al. [36] conducted a comparative experiment to study the effect of microwave-absorbent to pyrolyze HDPE using a microwave reactor. The absorbents used in this study were activated carbon and traditional coke. Although

both materials work well as microwave absorbents, the study reported that activated carbon showed more cracking across all temperatures and selectively produced lighter liquid oil products similar to petrol and diesel ranging from C_5-C_{21}. In another study, Undri et al. [37] explored microwave heating to pyrolyze HDPE and PP using two different absorbents, which were tires and carbonaceous char. HDPE using carbonaceous char as absorbent reported the highest liquid oil yield of 83.9 wt.% while PP reported 74.7 wt.%. However, using tires as absorbents, the solid char residue increased and accounted up to 33 wt.% while 0.4 wt.% for carbonaceous char. PP's pyrolysis liquid oil product reported more aromatic hydrocarbon while negligible aromatic hydrocarbon was found in HDPE liquid products.

Although microwave-assisted technology offers several advantages over conventional plastic pyrolysis, such as increased production speed, low temperature, and rapid, efficient heating, this technology has not matured yet. This technology needs further investigation with particular attention to finding low-cost materials that this technology demands.

2.3.3. Reactor Temperature

The reactor temperature is one of the most critical factors affecting the quality and quantity of pyrolysis products. Temperature dominates the plastic polymer cracking reaction, but not all the polymers can be cracked by increasing the temperature. Van der Waals force is the force between the molecules that attract and hold molecules together. When temperature increases in the pyrolysis process, the polymer absorbs the heat, and the molecule within the polymer begins to

vibrate. The Van der Waals force between the molecules collapses when the molecule's vibrations are high enough and start to evaporate from the surface of the polymer. The carbon chain breaks when the energy induced by the Van der Waals force along the polymer chains is greater than the enthalpy of the C-C bond in the chain [38].

The functioning of plastic polymer's thermal degradation can be measured using thermogravimetric analysis (TG). Many researchers have used this technique to study temperature in the plastic pyrolysis process. Different plastic polymers have other properties and degradation temperatures as their chemical structure changes from one plastic to another.

Polyethylene Terephthalate (PET) is a primary choice for plastic packaging for beverage and water bottles, food trays, electrical insulation, etc. It has a density of 1.38 g/cm^3, with a melting point over 250°C, the chemical formula is $(C_{10}H_8O_4)_n$, and the molecular structure is given in Fig. 2.3. PET has a poor thermal conductivity (i.e., 0.15 - 0.3 W/m*K) which causes challenges as the temperature controls the pyrolysis reaction's speed and selectivity [39]. Also, it contains heteroatoms that lead to the formation of undesirable oxygenated compounds.

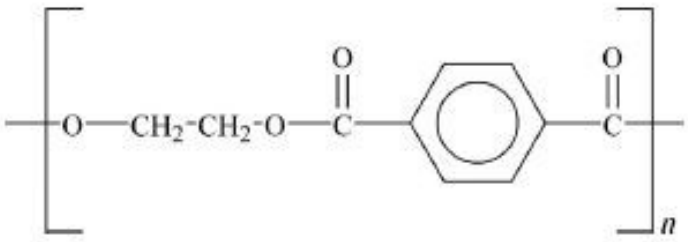

Fig. 2.3: PET molecular structure [40].

Many studies have been conducted to pyrolyze the PET polymer. Sarker et al. [41] conducted the PET pyrolysis study using calcium hydroxide as a catalyst. They started with the initial temperature for PET pyrolysis at 405°C and reported the onset temperature at 408.33°C with reference to a thermogravimetric analyzer (TGA) graph. Another study on the pyrolysis of PET was conducted by Cepeliogullar et al. [42]. In this study, PET fiber was pyrolyzed at several heating rates (5-20) Kelvin/min. They observed that PET degradation started at 400°C, and the slight change in the weight of PET occurred during the temperature in the range of 200-400°C. The maximum PET weight loss was reported at a temperature of more than 427.7°C, and no changes were observed at the temperature over 470°C. Hence, the author concluded that PET thermal degradation temperature ranges from 350-520°C.

High-density polyethylene (HDPE) is one of the most extensive plastic types found in MSW. It is majorly used in manufacturing containers, detergent bottles, etc. It is a long linear chain polymer. It has a density of 0.97 g/cm^3, with a melting point over 130.8°C, the chemical formula is $(C_2H_4)_n$, and molecular structure is given in Fig. 2.4. HDPE has a better thermal conductivity (i.e., 0.45-0.52 W/m*K) than other plastic polymers [39].

$$-CH_2-\ CH_2-\ CH_2-\ CH_2-\ CH_2-\ CH_2-\ CH_2-$$

Fig. 2.4: HDPE molecular structure [43].

HDPE is one of the most manufactured plastics, and therefore, a lot of research is done on the pyrolysis of HDPE. Sustaita-Rodriguez et al. [44] studied the thermal

stability and degradation mechanism of HDPE at different heating rates of 1°C/min and 10°C/min. They noticed that HDPE showed the highest thermal resistance. They reported that the first change based on the TGA curve observed at 375°C and 415°C for the heating rate of 1°C/min and 10°C/min, respectively. For the heating rate of 1°C/min, HDPE starts to degrade at 400°C, and total degradation occurs at 423°C whereas, for the heating rate of 10°C/min, HDPE starts to degrade at 415°C and completely degrades at 492°C. They suggested this could be because the degradation process at a low heating rate is an isothermal phenomenon that occurs over a long time, whereas at a high heating rate, it is a non-isothermal phenomenon. These conclude that the heating rate plays an essential role in the thermal degradation of plastic polymers.

Another study reported the thermal degradation of HDPE started at 378-404°C, and complete degradation occurs at 517-539°C based on the TGA at different heating rates of 10-50°C/min [45].

Low-density polyethylene (LDPE) is another plastic that has been manufactured widely. It is water-resistant and therefore widely used as plastic bags, wrapping material for packaging, trash bags, etc. As discussed in section 2.3.1, the LDPE has more branching than HDPE; therefore, it has a relatively lower density. It has a density of 0.910–0.940 g/cm^3, with a melting point over 130.8°C, the chemical formula is $(C_2H_4)_n$, and molecular structure is given in Fig. 2.5. LDPE has a better thermal conductivity (i.e., 0.33 W/m*K) than PET [39].

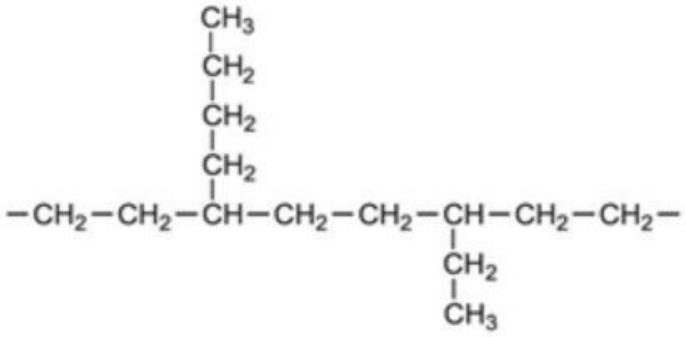

Fig. 2.5: LDPE molecular structure [43].

The research is conducted by Dubdub et al. [46] to study LDPE pyrolysis kinetics using TGA at the different heating rates of 5°C/min, 10°C/min, 20°C/min, and 40°C/min. They reported that the on-set temperature and complete degradation temperature gradually increased for increasing heating rate. Degradation started at 392°C, and total degradation occurs at 477°C for the heating rate of 5°C/min. Similarly, for the heating rate of 40°C/min, degradation started at 427°C, and complete degradation occurred at 521°C. Whereas Marcilla et al. [47] reported that a small amount of liquid oil product formation was started at 360°C - 385°C, and the maximum yield was obtained at 469°C-494°C.

Polypropylene (PP) is another linear chain hydrocarbon; therefore, it has a relatively lower density (0.895 – 0.92 g/cm³) than HDPE but has higher hardness and rigidity, making it more preferable for many in furniture, storage boxes, car parts, etc. PP has a poor thermal conductivity (i.e., 0.1 – 0.22 W/m*K), which causes similar challenges like PET as the temperature controls both the speed and selectivity of the pyrolysis reaction [39]. The melting point of PP is 160°C, the

chemical formula is $(C_3H_6)_n$, and the molecular structure is given in the following Fig. 2.6.

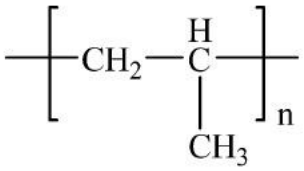

Fig. 2.6: PP molecular structure [48].

PP has a lower degradation temperature as compared to HDPE. Mandal et al. [49] have researched to study the thermal stability and degradation behaviour of various types of propylene and their mixture by using TGA analysis at four different heating rates 5, 10, 15, and 20°C/min over a temperature range of 40-550°C in the presence of nitrogen. They found that the primary decomposition of PP happened within the range of 350-490°C. It was observed that the first 5% weight loss of PP started at the temperature at 337°C, and complete degradation was achieved at 436°C. However, it was also reported that the degradation temperature increased with the increase in the heating rate. Another comparative study was conducted by Jung et al. [50]. This study examined the effect of temperature on the pyrolysis of HDPE and PP in a fluidized bed reactor using TGA and DTG analysis. It was found that the majority of HDPE and PP decomposition happened within the range of 400-500°C. However, it was observed that PP started to lose weight at a temperature below 400°C.

Polystyrene (PS) is made of styrene monomers, and the structure comprises a long hydrocarbon chain with a phenyl group connected to an alternate carbon atom.

It is heat resistant, and it offers sufficient durability, strength, and lightness that make this polymer desirable to be used in various sectors such as in the packaging of electronics, construction, medical appliances, and delicate machine spare parts. PS has a density within the range of 0.96–1.05 g/cm³ with a high melting point of 240°C compared to other plastic polymers. PS has poor thermal conductivity (i.e., 0.1-0.13 W/m*K), which causes similar challenges like PET and PP as the temperature controls both the speed and selectivity of the pyrolysis reaction [39]. The chemical formula is $(C_8H_8)_n$, and the molecular structure is given in the following Fig. 2.7.

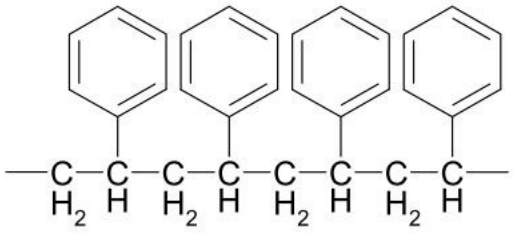

Fig. 2.7: PS molecular structure.

PS has the lowest degradation temperature in the pyrolysis process compared to other plastics. Abbas-Abadi et al. [51] investigated the pyrolysis of PS using a fixed bed and stirred reactor. Their study found that the degradation started at 329°C and was completed at a temperature 458°C. Similar results were concluded in another study conducted by Ding et al. [52]. This study observed that the PS thermal degradation occurs in a two-step. In the first step, a 6% mass loss of PS was observed within a temperature range of 200 - 260°C, and in the second step, complete degradation was observed within the temperature range of 350 - 450°C.

Thus, it is worth noting that the thermal degradation temperature of PS would be in the range of 350-500°C approximately.

The effect of temperature is more than just the degradation of plastic polymers. The temperature directly impacts both the quality and phase of the product as well. Mastral et al. [53] performed a critical experimental study to investigate the influence of temperature on the pyrolysis of HDPE in a fluidized bed reactor. The effect of the pyrolysis temperature on the product distribution is shown in Fig. 2.8. They observed that the overall gas product yield increased with increasing cracking temperature up to 730°C and the liquid product yield decreased with further increase in cracking temperature. However, above 850°C, the cyclization reactions formed aromatic hydrocarbon and gas product yield decreased.

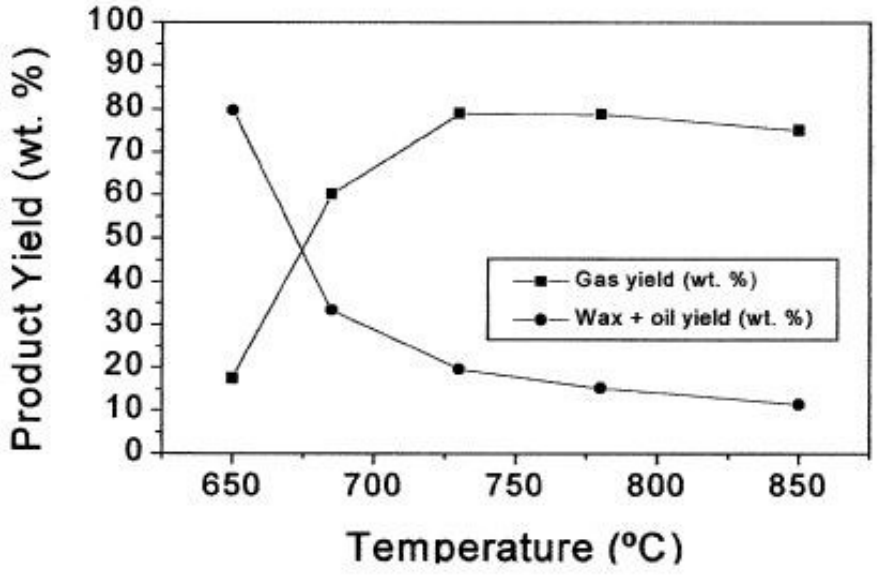

Fig. 2.8: Influence of the pyrolysis temperature on product distribution adapted from Mastral et al. [53].

2.3.4. Residence Time

Residence time, along with the pressure, is a temperature-dependent factor that directly influences the product distribution in the pyrolysis process. At a particular temperature, high residence time allows the feed in the reactor to absorb more heat than a low residence time. Therefore, low temperatures can be used at high residence time to achieve a similar extent of thermal degradation of plastics. The residence time of the raw plastic materials in the pyrolysis reactor can be defined as an average amount of time that particles spend in the reactor. Many studies have researched the effect of residence time in the pyrolysis process [53,54]. In a 2001 study, Mastral et al. [53] conducted a critical investigation to evaluate the influence of residence time on the pyrolysis of HDPE in a fluidized bed reactor. In this study, the residence time varied from 0.64 to 2.6s at five different temperatures. It was found that the yield of the wax product decreased with an increase in residence time at 640°C. At similar temperatures and residence time, the gas product yield increased. At high temperatures of 780°C, the product distribution changed, and the gaseous product yield increased to 86.4 wt.%, and liquid oil product yield decreased to 9.6 wt.% at 1.34 s. Therefore, at longer residence time, the conversion of the gaseous product increases that are lower molecular weight hydrocarbons and non-condensable gases.

Another study was conducted by Onwudii et al. [54] to investigate the effect of temperature and residence time on the pyrolysis of LDPE and PS in a closed batch reactor. It was reported that the degradation of LDPE yielded 91.1 wt.% oil and 8.7 wt.% of gaseous products within a time at which pyrolysis reaction temperature

reached 450°C and was considered a zero-residence time. However, with an increase in residence time to 120 min, the liquid oil product yield drastically reduced to 61 wt.%, whereas the gaseous product yield increased to 28.5%. The long residence time allows further cracking of liquid oil to gas, resulting in high gas production.

2.3.5. Reactor Pressure

A high-pressure environment elevates the boiling point of hydrocarbon compounds. Products with elevated boiling points are further pyrolyzed during such pressurized conditions. As most researchers conducted their investigation at atmospheric pressure, very few studies investigated the effect of pressure on the pyrolysis process. However, Murata et al. [55] conducted an experiment to examine the impact of pressure on the thermal degradation behaviour of HDPE in a stirred tank reactor under elevated pressures ranging from 0.1 to 0.8 MPa. Higher pressure shifts their molecular weight distribution to an even lower molecular weight. The effect of pressure on carbon number and their weight fractions in the pyrolysis products of PE at different temperatures is shown in Fig. 2.9 and Fig. 2.10.

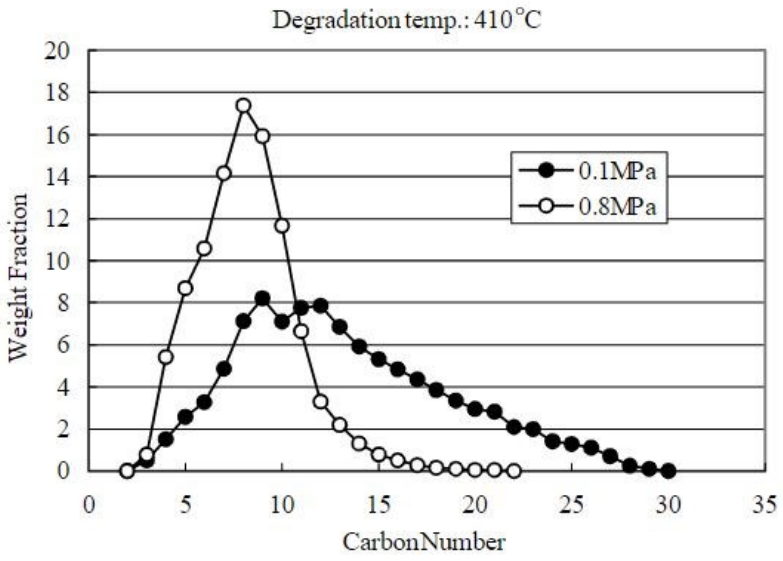

Fig. 2.9: Effect of pressure on carbon number distribution adapted from Murata et al. [55].

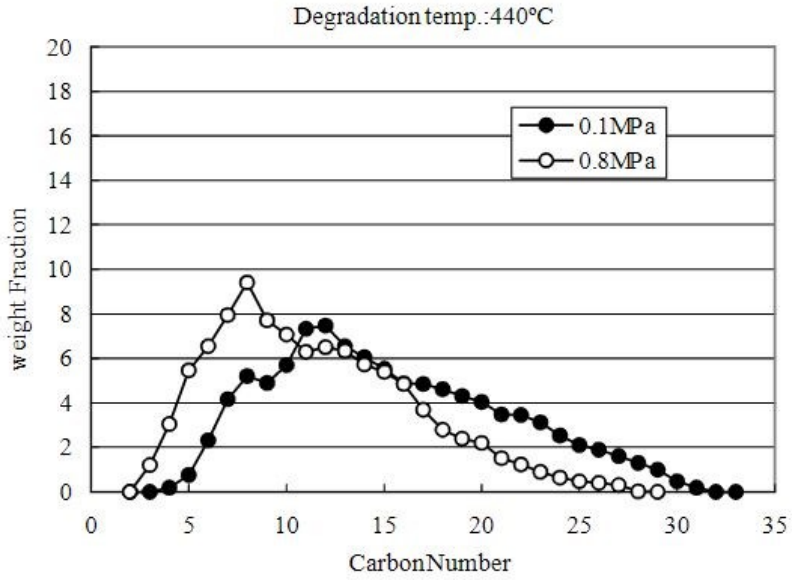

Fig. 2.10: Effect of pressure on carbon number distribution adapted from Murata et al. [55].

They observed that the gaseous product yield increased from 6 wt.% to 13 wt.% at 410°C and from 4 wt.% to 6 wt.% at 440°C. Fig. 2.11 shows the gaseous product yield during thermal degradation at different pressures. It can be seen from the figure that the yield of the gaseous product increases with the increase of pressure [55].

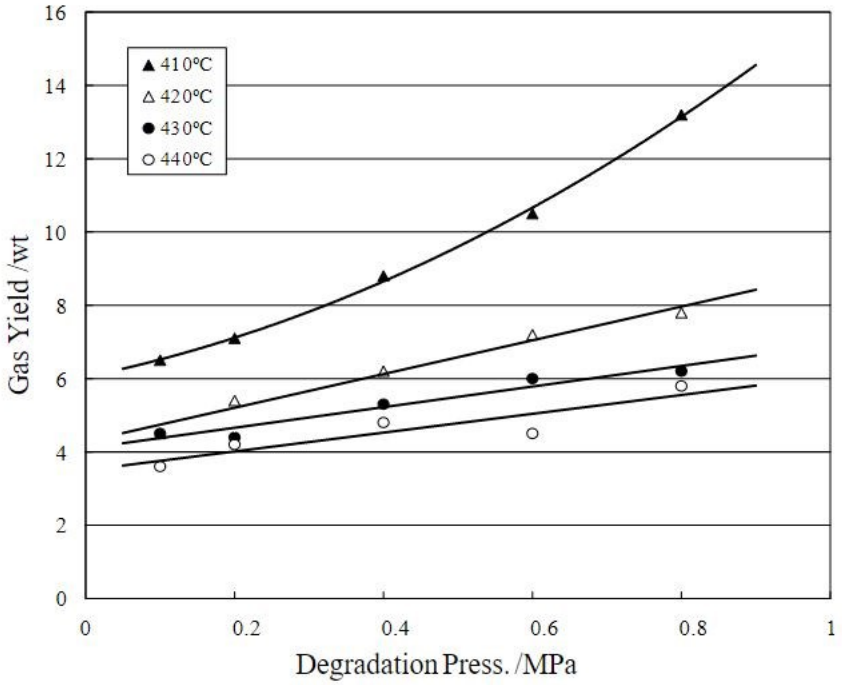

Fig. 2.11: Effect of pressure on the yield of gaseous product adapted from Murata et al. [55].

They reported that pressure directly affects the scission of the C-C link of the polymers during the thermal degradation. Therefore, the pressure significantly impacts the rate of double bond formation. They further concluded that the rate of double bond formation decreased with an increase in pressure [55].

3. Previous Work on the Simulation of MPW Pyrolysis Processes

Due to the importance of the plastic pyrolysis process as a tool in utilizing plastic waste to produce fuel, the literature available in this area is extensive. However, most of the published work is focused on lab-scale experimental studies that investigate the plastic pyrolysis process, and only a few process simulation studies are available in the literature [56–64]. In this section, an in-depth analysis of all previous investigations is presented. Their accomplishments are highlighted, and the differences in the prediction methods and results are explained.

3.1. Introduction and Background

As mentioned in the previous sections, pyrolysis promises to be a cost-effective and environmentally-friendly approach for managing the rapidly-increasing problem of handling Municipal Plastic Waste, MPW. The techno-economic performance of such operations can be well assessed using process simulation methodologies and tools. However, the relevance of results obtained is a strong function of how well each unit involved is simulated and how well the interaction between the various units is represented. Therefore, a literature search was undertaken using different databases (Google Scholar, Engineering village, ScienceDirect and ACS publication), and only 9 references were identified in the period 2014 to March 2022. These are listed in Table 3.1 according to their chronological order. That table also summarizes the corresponding simulation information regarding the feedstock used, its feed rate, and the operating conditions. Results obtained from all these investigations agree that the overall technical and economic performance of the MPW pyrolysis process is affected by:

1. The accuracy by which the feedstock and its feed rate are specified.
2. The accuracy by which the thermodynamic properties of the various constituents (gas, liquid, and solids) are estimated. This applies to the individual components and mixtures thereof, over the whole range of operating conditions encountered in the process.
3. The accuracy by which the performance of the pyrolysis reactor and the liquid fractionation unit (if included) are simulated. These items are particularly important as they represent the heart of the process and strongly affect its overall technical and economic performance.

Finally, no matter how precise and accurate the process simulations are, confidence in the predicted results will always remain in doubt unless they closely match the experimental results obtained under the same conditions (preferably developed using pilot-scale or full-scale operations).

A summary of the simulation methodology used in the published papers/reports is presented in Table 3.2. As can be seen from the information presented in this table, initial efforts attempting to simulate the performance of the MPW pyrolysis process were undertaken using process simulation software packages (e.g., Aspen Plus® and Aspen HYSYS®). Aspen modules for both the reactor and separation units and the thermodynamic property method for accurate estimation of various constituents are also presented.

Furthermore, the software should have the ability to accurately predict the physical properties of the various streams encountered in the process and how they are affected by changes in operating conditions (mainly temperature and pressure in

the case at hand). In this regard, the software used, Aspen Plus®, is considered to be the most suitable software and, as shown in Table 3.2, was used by the majority of previous investigators.

Peng Robinson is a thermodynamical property method used by most investigators, as presented in Table 3.2, because it is more suitable for gas and condensate in hydrocarbon systems, explained briefly in section 5.1.1. The type of reactor module used is also essential. There are many standard modules available for the reactor in Aspen Plus® and Aspen HYSYS® software that differs in functionality because of the equation used in the calculations.

Table 3.1: Summary of plastic pyrolysis simulation conditions and methodologies used

Reference	Feedstock	Feed rate (kg/hr)	Operating Temp. (°C)	Operating Pres. (atm)	Process simulation software	Thermo. property package	Reactor simulation module	Distillation simulation module
Sahu et al. [56]	40% PE, 40% PP, & 20% PS	1142	500	1	Aspen Plus®	n.p.	n.p.	Flash2
Alla et al. [57]	30% PE, 30% PP, & 40% PS	100	450	1	Aspen HYSYS®	n.p.	n.p.	Flash2
Moses et al. [58]	100% HDPE	2000	450	n.p.	Aspen HYSYS®	n.p.	Conversion	Flash2
Adeniyi et al. [59]	100% LDPE	10	450	1	Aspen HYSYS®	Peng-Robinson	CSTR	Flash2
Fivga et al. [60]	Mixture of PE, PP, & PS	100	530	1	Aspen HYSYS®	Peng-Robinson	RYield	Flash2
Deng et al. [61]	MSW	1.32	500	1	Aspen Plus®	Redlich-Kwong-Soave	RYield	Sep2

Reference	Feedstock	Feed rate (kg/hr)	Operating Temp. (°C)	Operating Pres. (atm)	Process simulation software	Thermo. property package	Reactor simulation module	Distillation simulation module
Jiang et al. [62]	31.25% LDPE, 31.25% HDPE, 7.29% PP, 13.5% PS, 11.46% PVC, 5.25% PET	1000	500	n.p.	Aspen Plus®	n.p.	RStoic	Sep2
Selvagana pathy et al. [65]	3 cases:100% PE, 100% PP, 100% PS	100	450	1	Aspen HYSYS®	Peng-Robinson	Conversion	Flash2
Lameh et al. [64]	100% HDPE	150	520	0.987	Aspen Plus®	Peng-Robinson	Furnace + User2 block	RadFrac
Present study	20.4% PE, 71.4% PP, & 8.2% PS	500	440	0.998	Aspen Plus®	Peng-Robinson	RYield	RadFrac

*Flash2: Two-outlet flash separator

*Sep2: Two-outlet component separator

*RadFrac: Rigorous fractionation/distillation

*User2: User-defined function block

*n.p.: Not Provided in the literature.

The earliest study was conducted by Sahu et al. [56]. They used process simulation to perform a technical and economic feasibility assessment for a catalytic cracking unit operating continuously at the rate of 1,142 kg/hr capacity waste plastics to produce fuel oils in Malaysia. The reactor temperature was taken to be 500°C operating under atmospheric pressure conditions. The plastic waste feedstock was assumed to be 40% PE, 40% PP, and 20% PS.

They used several key simplifying assumptions:

1. No pressure drop was considered across the equipment in the entire process.
2. No heat losses were considered.

Critical information such as thermodynamic properties and the reactor module type was not provided. Their economic analysis suggested that the proposed approach is economically feasible for a plant with an annual feed capacity of 120,000 tons, provided that the light fuel oil and heavy fuel oil produced can be sold at prevailing 2013 gasoline and diesel prices. Production profit was assumed to be $0.481/L. The initial investment cost was estimated to be around $58.6 million.

Alla et al. [57] simulated a 100 kg/hr plastic waste pyrolysis process using Aspen HYSYS® software at 450°C and atmospheric pressure. Critical information such as thermodynamic properties and the reactor module type was not provided. Although the plastic waste feedstock was considered a blend of 30% PE, 30% PP, and 40% PS, it was modeled as ethylene, propylene, and styrene. They found that their process does not require an external heating source since the thermal heating

requirements were found to be about one-third of those generated by burning the pyrolysis oil and gases. The experimental performance data was not provided, and no comparison was made between their simulation results with the experimental data.

Moses et al. [58] used Aspen HYSYS® software to simulate a power plant fueled by plastic waste pyrolysis products (2000 kg/hr of 100% HDPE with the pyrolysis reactor operated at 450°C). A simple Aspen HYSYS® conversion reactor module was used to simulate the pyrolysis reactor, with its reaction conversion being based on the pyrolysis reaction used by Alla et al. [57] to develop their Aspen HYSYS® model. Unfortunately, critical information such as the thermodynamic properties and the pressure at which the reactor was operated were not provided. However, their predicted liquid fuel oil yield (55.5%) was significantly less than that was reported by Alla et al. [57] (liquid oil yield was 95.3%).

Adeniyi et al. [65] developed a simulation model for a plastic pyrolysis plant (10kg/hr capacity of 100% LDPE feedstock). The performance of the pyrolysis reactor was simulated using the Aspen HYSYS® CSTR reactor (operating at 450°C and atmospheric pressure) with its reaction conversion being based on the pyrolysis reaction used by Alla et al. [57]. They used the Peng-Robinson thermodynamic property method in their simulation and predicted the effect of reactor temperature on the reaction conversion. Their predicted liquid oil yield was 92.88% which is much closer to the liquid yield reported by Alla et al. [57]. They also suggested that their product composition is consistent with the experimental results available in the literature.

Fivga et al. [60] investigated the technical and economic feasibility of a 100 kg/hr plastic waste pyrolysis plant using Aspen HYSYS® software. The pyrolysis reaction was assumed to take place in an inert atmosphere, at atmospheric pressure, and fixed reaction temperature of 530°C. The feedstock of plastic waste was modeled by considering an elemental composition (85 wt.% carbon and 15 wt.% hydrogens) based on a dry ash-free basis. The Aspen HYSYS® RYield reactor module was used to simulate the pyrolysis reactor using Peng-Robinson thermodynamic property method, with its performance being based on the findings reported by a recycling company based in the UK. They reported that the process does not require an external heating source (e.g., natural gas) since the thermal heating requirements are about one-quarter of those generated by burning the pyrolysis char and gases. They reported that a 100 kg/hr capacity plant could be economically feasible, but no comparison was made of the Aspen HYSYS® predictions with the actual fuel composition.

Deng et al. [61] conducted a study to predict and analyze the MSW pyrolysis and gasification process in an up-draft fixed bed by using the Aspen Plus® software. They used the Redlich-Kwong-Soave (RKS) thermodynamic property method in the simulation model to analyze the performance parameters, including syngas composition, gasifying temperature and carbon conversion rate. The Aspen Plus® RYield reactor module was used to simulate a pyrolysis reactor, with its performance being based on the findings reported by Luo et al. [66]. The pyrolysis unit operated at 550°C under atmospheric pressure for an MSW feed capacity of 1.32 kg/hr. They made the following critical assumptions:

1. Steady-state operation with no pressure drop across any equipment in the process and no heat losses.
2. The feedstock of MSW was modeled by considering an elemental composition.
3. MSW particles were assumed of uniform size and temperature.

They found that their predicted gas yields were in good agreement with the experimental data reported in the literature. Their simulation results found that the mixture of flue gas and water vapour as gasifying agents is the most economical and green method to obtain a better carbon conversion rate. They considered reaction kinetics only for the gasifying unit and not for the pyrolysis unit.

Jiang et al. [62] conducted an exciting process simulation using molten solar salt as the heating medium for pyrolysis of mixed plastic waste containing PVC. They used the Aspen Plus® RStoic reactor module to simulate the pyrolysis reactor, which was operated at 500°C and 1 atm. They used the electricity generated from the non-condensable pyrolysis gas as the energy source for the pyrolysis process, and the converting efficiency of gas-to-electricity is about one-third. They further reported that energy required for pyrolysis (605 kW) was less than the electricity generated (662 kW) from the combustion of the non-condensable gases, claiming that their pyrolysis process can be self-sustained. They also reported that for a plant capacity of 8000 t/yr, the solar power integration adds extra equipment cost, which increases the total capital investment by 1 million and decreases the return on investment by 3.5%. The solar power integration will become profitable only

when the solar energy is more than 50% of the energy required to operate the plant of capacity 8000 t/yr or when the electricity price increases.

The most recent study was conducted by Lameh et al. [64] and used process simulation to investigate the integration of concentrated solar power with the pyrolysis of HDPE operating continuously at the rate of 150 kg/hr. The feedstock of plastic waste was modeled by considering a single elemental composition (85.81 wt.% carbon, 13.86 wt.% hydrogens and nitrogen 0.12 wt.%) based on a dry ash-free basis. They combined Aspen Plus® Furnace with a User-defined block function module (User2) to simulate the pyrolysis reactor, which was operated at 520°C and 0.987 atm. The Furnace module was used to define sensible heat of HDPE, and User2 was used to define reaction kinetics that was developed by Levine et al. [67]. They suggested that the integration of solar energy with the HDPE pyrolysis process would provide 52.5% of the total energy requirement of the pyrolysis process annually, and in summer, 72.6% of the total energy requirement could be generated using solar energy. They used the Aspen Plus® RadFrac module to simulate the distillation unit and predicted that the total oil yield was 52.9%, gases was 25.1%, and the rest was char 21.9%. The experimental performance data was not provided, and no comparison was made between their simulation results with the experimental data.

3.2. Limitations of Present Body of Knowledge

The in-depth analysis of the literature pertaining to the simulation of MPW pyrolysis processes suggests that the following factors need to be considered: operating temperature, operating pressure, reaction kinetics, type of reactor module,

thermodynamical property package and feed composition. These factors have a significant impact on the pyrolysis process simulation. The following discussed process simulation studies had provided great insight into the viability of the plastic pyrolysis process at the commercial scale and provided strong economic conclusions.

However, these simulation studies do not address many of the detailed technical aspects of the plastic pyrolysis process. Most process simulation studies of plastic pyrolysis have modeled the waste plastic feedstock by considering an elemental composition (e.g. 85 wt.% carbon and 15 wt.% hydrogens) based on a dry ash-free basis [60–62,64]. Other studies have used typical organic monomer compounds such as styrene, ethylene, and propylene for polystyrene, polyethylene, and polypropylene [57,58,65]. This approach does not give a proper estimation of polymer properties; for example, the melting point of ethylene is -169.2°C, and polyethylene is 115°C. It is particularly essential for the reactor modules such as RStoic, RGibbs and CSTR in Aspen Plus, where reaction stoichiometry is critical for developing the process model. Adeniyi et al. [59] used an approach where the LDPE was added as a hypothetical component using LDPE properties like density, molecular weight and normal boiling point. Sahu et al. [56] used real polymers components that are available in the component library of the polymer template of the Aspen Plus®.

The selection of the reactor module depends on the availability of data. RStoic in Aspen Plus® and Conversion Reactor in Aspen HYSYS® are used when reaction stoichiometry and conversion or molar extent for each reaction is known, and

reaction kinetics are unknown or unimportant. Both Moses et al. [58] and Selvaganapathy et al. [65] used the Aspen HYSYS® Conversion reactor module to simulate the same stoichiometric reaction. However, no discussion was provided from the literature that supports the selection of reaction stoichiometry that was used in their study. Similarly, Jiang et al. [62] used the Aspen Plus® RStoic reactor module; however, no reaction stoichiometry or reaction kinetics were provided. RYield reactor module is considered the most suitable reactor module and, as shown in Table 3.2, was used by some previous investigators. RYield reactor is considered when the reaction stoichiometry or kinetics is unavailable or cannot be used, but the product yield is available. In the present study, the RYield reactor is used and discussed in detail in section 5.1.2.

The Table 3.2. represents the simulation methodologies used in the literature. In most studies, the Aspen Flash2 separator module was used [56–60,65], while in two studies, the Sep2 separator module was used for distillation [61,62]. The Flash2 module is used for flashes, evaporators and single-stage separators, whereas the Sep2 is used for distillation and absorption when the details of separation are unknown. These separation modules are not robust and do not predict the performance of the distillation in detail. In the present study, the RadFrac column used has a more rigorous rating and design of the distillation column and, therefore, predicts the actual distillation performance.

In many studies, no attempts were made to compare predicted results with existing literature or with experimental data [56,57,60,62,64,65]. Moses et al. [58] compared their simulation results to reported data in existing literature, which they

found to be different. Deng et al. [61] verified their simulation results with experimental data reported in the literature, which they found to be in agreement. Jiang et al. [62] provided a comparison of the economic predictions with the reported data in the literature. In the present study, the simulation results were compared to the experimental data and to the existing literature data.

Although few process simulation studies have investigated economic analysis [56,60,62,64], to the best of our knowledge, there was no study that conducted a technical sensitivity analysis of the plastic pyrolysis process. Furthermore, no study was found in the literature related to optimizing the distillation unit of a plastic pyrolysis process. Technical sensitivity analysis can optimize the process that ultimately affects operation cost and the return on investment.

4. The Sustane Pyrolysis Process

The following section provides the background and general information about the MPW pyrolysis process plant located at Sustane Technologies Inc., Chester, Nova Scotia.

Sustane is attempting to utilize the MSW in Chester, NS, to produce valuable products while simultaneously reducing carbon emissions into the environment. The MSW is passed through a series of thermal conditioning and separation sections that separate glass and sand, metals, biomass, and MPW, as shown in fig. 4.1.

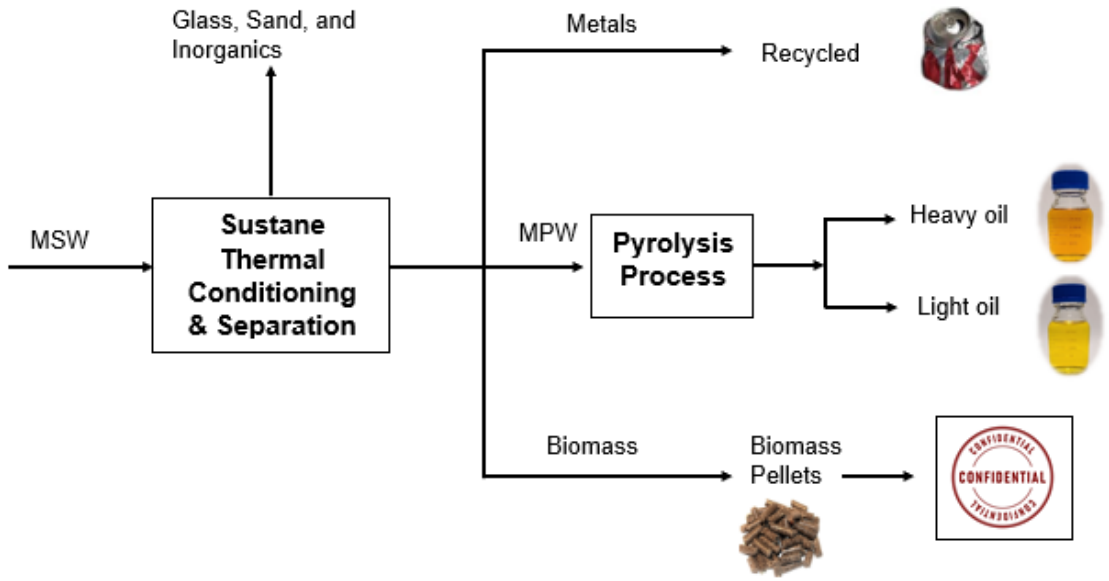

Fig. 4.1: Sustane Ultimate Waste Circular Process

As indicated in Chapter 3, the confidence placed on the results obtained using any process simulation study is very limited until its predictions can match the actual performance of full-scale or pilot-scale units. Therefore, this investigation is fortunate to have access to performance results obtained from Sustane, Chester Plant, which sorts out MSW into biomass, metals, and waste plastic. The sorted out MPW is then further converted to liquid fuels and non-condensable gases.

4.1. Sustane Technologies Inc. Process For Pyrolyzing MPW

Oil fuels have a high economic value as they can be sold as feedstock to a petrochemical company (where they can be used to produce plastic again) or blended with the feedstock of petroleum refineries. The produced non-condensable gases are used to run boilers for the MSW separation process, and any excess gases are disposed of in the flare. The block flow diagram and process flow diagram are shown in Fig. 4.2 and Fig. 4.3, respectively.

The Sustane plastic pyrolysis process is divided into two main sections:

1. Reactor section: consists of three pyrolysis reactors (two primary rectors and one secondary reactor) partial condensers.
2. Distillation section: consists of two distillation columns.

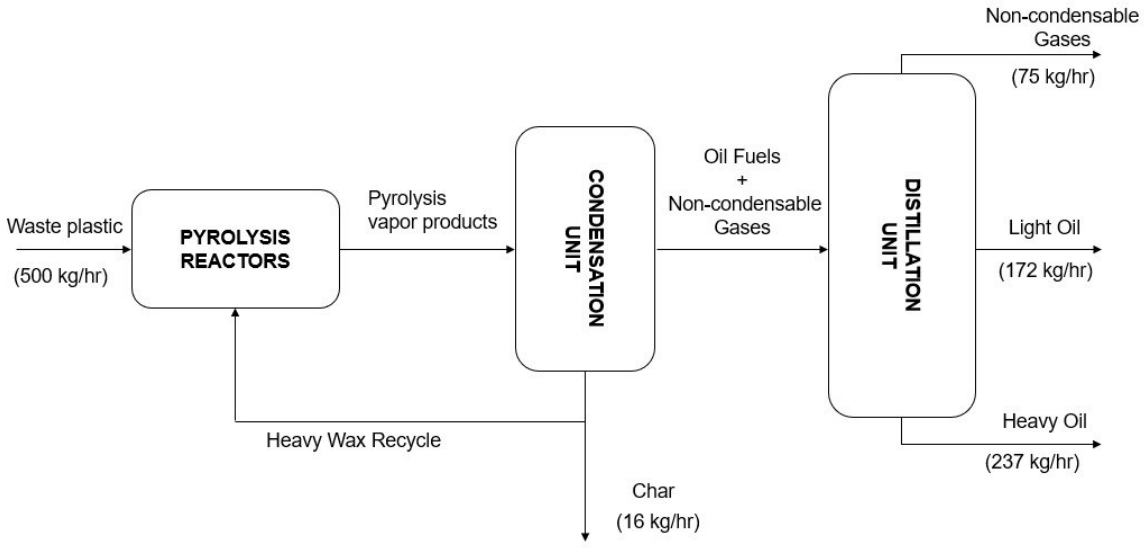

Fig. 4.2: Plastic pyrolysis block flow diagram

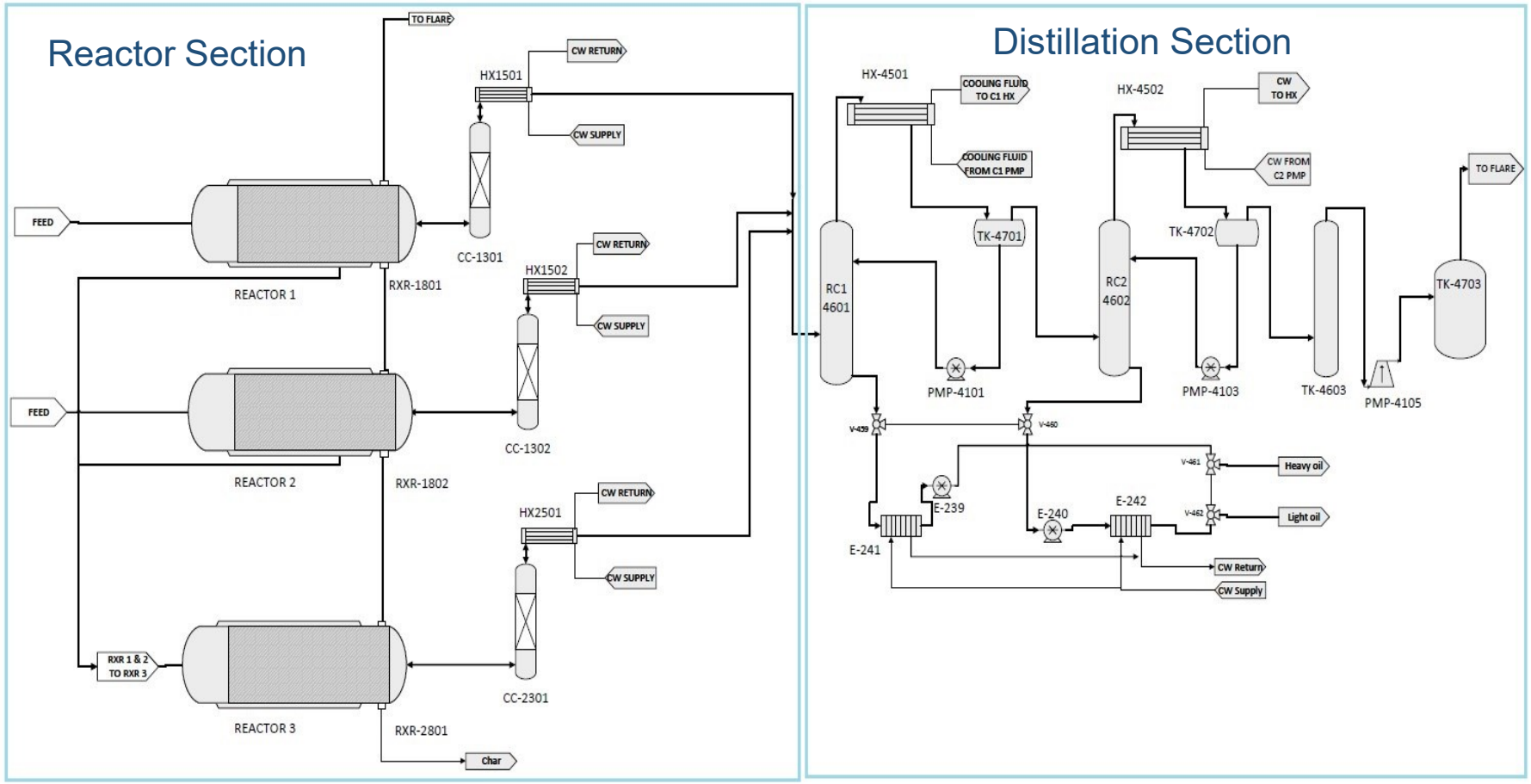

Fig. 4.3: Continuous waste plastic pyrolysis process flow diagram.

4.1.1. Reactor Section

The plastic pyrolysis process takes a mixed MPW stream that has been sorted, cleaned, dried, and shredded to a maximum of 6mm flake using Sustane' proprietary process. During the start-up, the reactors are purged with nitrogen to eliminate oxygen before the shredded MPW is introduced into the reactor section via a plastic extruder.

The three pyrolysis reactors include two primary reactors (RXR-1801 and RXR-1802) and a secondary reactor (RXR-2802). The primary reactors operate in parallel to handle the desired production capacity, and the secondary reactor further pyrolyzes the unreacted plastic and heavy wax products from the primary reactors.

All reactors operate at 440°C and slightly under atmospheric pressure. Reactors use the heat generated by burning non-condensable gases produced from the pyrolysis process plant to reach a cracking temperature of 440°C.

At 440°C, MPW undergoes a series of reactions of radical chain mechanisms, where initiation, propagation (transfer and decomposition), and termination reactions occur. These reactions crack the longer hydrocarbon chains into smaller chain molecules that make up fuel products. These fuel products are comprised of carbon number from 1 to 20 or up to 30. The carbon number from 1 to 5 are non-condensable gases such as methane, the chains from 5 to 12 are Naphtha, 12 to 20 are Diesel and 20+ are heavy wax [68].

These gaseous reactor products are cooled from 440°C to 330°C in three partial condensers, which are the combination of condenser columns (CC-1301, CC-1302 and CC-2301) and coolers (HX-1501, HX-1502 and HX2301). Each partial condenser is dedicated to a primary and secondary reactor.

Lighter constituents (light and heavy oil vapours and non-condensable gases) are sent to the distillation unit for fractionation. The heavy wax is condensed and returns to the reactors after flowing counter-current against the rising pyrolysis vapour products to enhance the stripping of non-condensable gases, heavy oil and light oil.

4.1.2. Distillation Section

The mixture of light and heavy oil vapours and non-condensable gasses from the partial condensers are fractionated in the distillation unit.

The distillation unit comprises two distillation columns (RC-4601 and RC-4602) that operate under a vacuum. The heavy oil vapour is fractionated in the first distillation column (RC-4601) that operates at 0.985 atm with a column pressure drop of 0.01 atm and a distillation column bottom temperature of 155°C. Heavy oil is collected from the bottom of the distillation column (RC-4601).

The light oil vapour is fractionated in the second distillation column (RC-4602) that operates at 0.97 atm with a column pressure drop of 0.01 atm and a distillation column bottom temperature of 90°C. Light oil is collected from the bottom of the distillation column (RC-4602).

After the distillation column RC–4602, the remaining gases, such as propane, ethane, and methane, are non-condensable under normal conditions. These non-condensable gases are compressed and stored. They are used as an energy source to heat the pyrolysis reactors and boilers in the MSW separation process. Any extra non-condensable gases that cannot be stored are fed to flare assembly, where they are combusted.

4.2. Process Performance

The present simulation study of the plastic pyrolysis process of Sustane incorporates three types of data: material composition, physical properties, and reaction conversion data.

At Sustane, plastic waste goes through a series of mechanical separation processes. The composition of MPW fed to the reactors is continuously monitored and controlled by an infrared (NIR) sensor for the waste sorting system manufactured by TOMRA, a Norwegian multinational corporation. As noted in section 2.3.1, some plastics such as PVC and PET are removed and not pyrolyzed because the presence of chlorine and oxygen atoms can result in the formation of chlorinated and oxygenated compounds harmful to human health and the environment. Therefore, the final average plastic waste composition that is fed into the pyrolysis reactor is as follows:

Polypropylene: 71.40%

Polyethylene: 20.40%

Polystyrene: 8.20%

The physical properties such as temperature, pressure, and other parameters represent real-time data from the pyrolysis plant from Sustane's Chester facility. Each of the two primary reactors has a feed rate of 250 kg/hr, and therefore the total design capacity of the pyrolysis reactors is 500 kg/hr. The critical operating parameter for the reactor unit is presented in the following Table 4.1.

Table 4.1: Operating parameter for Reactors.

	Primary Reactors		Secondary Reactor
	RXR-1801	RXR-1802	RXR-2801
Temperature (°C)	440	440	440
Pressure (atm)	0.998	0.998	0.998
Mass Flows (kg/hr)	250	250	60

Reactors use the heat generated by burning non-condensable gases produced from the pyrolysis process plant. On average, the total production of non-condensable gases is within a range of 15-20% (85 - 100 kg/hr) of the total MPW feed rate. The limitation related to collecting samples of these gases is discussed in section 4.3. The estimated operating parameters are given in table 6.1.

The two liquid products have a high economic value. Light oil holds higher economic value than heavy oil as it nearly resembles naphtha that requires less processing for petrochemical companies to reuse it again to produce plastic and other chemicals. The heavy oil samples are collected from the bottom outlet of the

first distillation column (RC-4601). On average, the total production of heavy oil is within a range of 45-50% (225 - 250 kg/hr) of the total MPW feed rate. The operating parameters for heavy oil are given in Table 6.1.

The light oil samples are collected from the bottom outlet of the second distillation column (RC-4602). On average, the total production of light oil is within a range of 30-35% (150 - 175 kg/hr) of the total MPW feed rate. The operating parameters for light oil are given in Table 6.1. The Aspen Plus® predicted and experimental composition of light oil is presented and compared in Appendix A.1.

4.2.1. Data Samples

The design, parameters and operating conditions of Sustane's Pyrolysis plant were used to simulate the current research.

The plant has 3 products: non-condensable gases, solid char, and liquid fuels. Liquid fuels have much higher economic value and are the focus of the research. There are two types of liquid fuels produced at the plant a) Light oil and b) Heavy oil.

In order to assess the ability of the simulation models discussed in section 5 and to reliably predict the actual performance of Sustane's pyrolysis process, samples of light oil and heavy oil, as well as the solid char product, were collected. The light oil and heavy oil sample collection were done twice under practically the same operating conditions, as shown in Table 4.1. However, due to limitations that would require the dismantling of process equipment, only one char sample was collected under these operating conditions. The gaseous stream generated by the process

was not examined because of the lack of a sample collection facility and flammable nature of the gases, which would create occupational health and safety concerns at the plant location.

In total, 5 samples were analyzed: two samples of light oil and two samples of heavy oil from the two experimental runs and one char sample following the completion of the second experimental run.

Finally, the char and pyrolysis fuels such as heavy oil and light oil were characterized by performing Gas Chromatography with Mass Spectrometry (GC-MS). The analyses were performed by Mr. Zhehan Jiang and Dr. Suzanne Budge from the Marine Lipid lab Dalhousie University.

They analyzed samples using a gas chromatograph model Trace 1310 from Thermo Scientific coupled with a single quadrupole mass spectrometer model ISQ 7000 from Thermo Scientific.

The GC injector and transfer line temperature were set at 280°C, and the injector operated in split mode with a 20:1 split ratio. The carrier gas was helium with a constant flow of 1 ml/min. A ZB-5 capillary column (30m × 0.25mm i.d., 0.25μm film thickness) manufactured by Phenomenex (USA) was used. The oven temperature program was started at 30°C and held for 10 min, ramped at 2.5°C/min to 70°C and was held for 1 min, ramped at 8°C/min to 150°C and was held for 1 min, ramped at 15°C/min to 280°C and held for 5 min with a total time of 49.6 min.

The MS was operated at the same ion source and transfer line temperature of 300°C with electron ionization (EI) mode. The identification of compounds was based on the National Institute of Standards and Technology (NIST) mass spectrum library.

5. Development of Detailed Pyrolysis Process Simulation

5.1. Crude Characterization

In order to simulate the process and understand the results effectively without diminishing the physical properties of the fuel oils, the components list needs to be shortened. It is challenging to incorporate a large number of experimental components into the simulation model and conduct the technical sensitivity and optimization analysis. Therefore, characterizing the component is essential to shorten the list. There are two methods for crude characterization:

1. Characterization based on carbon number of components
2. Characterization based on the boiling point of components

The GC/MS analysis obtained more than 250 components. Many components have similar carbon numbers but different boiling points and vice versa. For example, many C_{13}-C_{19} components were a combination of acetate, alcohol, and alkenes with a significant boiling point range. Many C_{13}-C_{15} compounds have similar boiling points to C_{11}/C_{12}, while other C_{15}/C_{16} molecules had boiling points similar to C_{20}. The significant variation of boiling points across compounds with similar carbon numbers precluded the use of carbon number as the primary method for reducing the number of components included in the simulation..

Whereas in the crude characterization on the basis of the boiling method, the group of chemical compounds with very equivalent or close boiling points are represented as a single component. While this may not capture some of the viscosity modifying characteristics of some complex molecules, boiling point-

based approaches are standard practice for crude characterization across the chemical industry when thermal separation methods like distillation are of interest.

One of the main objectives of this work is to optimize the distillation unit to maximize the light oil and heavy oil production rate and closely predict the physical properties such as density, viscosity, and flash point. Furthermore, the distillation column works on the basis of vapour-liquid equilibrium, pressure, and true boiling point (TBP) curve of the chemical compound. Thus, to simulate the entire process better and develop an accurate understanding of the results, crude characterization on the basis of a point is a better method; therefore, it is used in the present work.

5.2. Component List

On average, the total production of non-condensable gases is within a range of 15-20% (85 - 100 kg/hr) of the total MPW feed rate. Whereas the total production of heavy oil is within a range of 45-50% (225 - 250 kg/hr), and light oil is within a range of 30-35% (150 - 175 kg/hr) of the total MPW feed rate. The char is 3-5% of the total MPW feed rate.

The component list for reaction conversion yield is prepared in the following two steps:

1. An average of GC/MS results of light oil, heavy oil and char is taken. The components are then characterized based on boiling point.
2. Reaction conversion yield data is prepared based on a given product range, such as 15-20% non-condensable gases, 75-85% liquid oils and 3-5% char.

The reaction conversion yield date is presented in given in Appendix A.1. It is worth noting that this work focused on the average composition obtained from limited sampling of experimental results, and may not reflect the range of reactor outlet compositions which could result from the pyrolysis reactor.

5.3. Model Development

The present simulation study is conducted to simulate the plastic pyrolysis process of the Sustane Technologies Inc. Chester plant and analyze and optimize the results such as material and energy balances for each process equipment and their operating conditions. A non-stoichiometric steady-state model was developed to simulate the plastic pyrolysis process using the Aspen Plus® version 10 process simulator. Aspen Plus® is considered to be the most suitable software and, as shown in Table 3.2, was used by the majority of previous investigators. Model development requires defining the chemical components, appropriate thermodynamic property package, equipment modules, and operating conditions.

In the following section, the process simulation model developed for the plastic pyrolysis process is discussed in detail:

5.3.1. Simulation File and setting

Within Aspen Plus®, it is essential to use a suitable simulation template to conduct a technical analysis of a chemical process, develop a process model, and carry out a simulation study. There are 11 simulation templates available in Aspen Plus®. The generic (blank simulation) template in Aspen Plus® is used by most previous investigators discussed in section 3.2 but does not contain polymers such as

polyethylene. The use of a generic template limits the scope of the simulation and requires many assumptions. However, Sahu et al. [56] have used the Aspen Plus® polymer template that allows using real polymers such as polyethylene. Therefore, in the present simulation study, the Aspen Plus® polymer template is used, eliminating the need for assumptions related to the MPW feed.

The second step for estimating the process from a thermodynamic perspective is choosing an appropriate thermodynamical property package, i.e., equation of state (EOS). Peng Robinson (PR) is a thermodynamical property package used by most investigators, as outlined in Table 3.2.

The PR property package uses the alpha function, which makes it suitable for hydrocarbon processing applications such as gas processing, refinery, and petrochemical. This alpha function predicts the thermodynamical properties such as vapour pressure of specific chemical compounds at reduced temperatures, as presented in equation (2). The PR can also accurately model polar, non-ideal chemical systems. Therefore, PR thermodynamical property package is used in the current simulation.

The standard form of the PR equation of state is given by:

$$P = \frac{RT}{V_m - b} - \frac{a(T)}{V_m(V_m + b) + b(V_m - b)}$$

$$a(T) = \alpha a(T_C)$$

$$a(T) = 0.45724\ \alpha \frac{R^2 T_c^2}{P_C}$$

$$b = 0.07780 \frac{RT_C}{P_C}$$

$$\alpha = \left(1 + k\left(1 - \sqrt{T}/T_C\right)\right)^2 \quad (2)$$

$$k = 0.37464 + 1.5422\omega - 0.26992\omega^2$$

Where: P = Pressure (Pa)

V = Molar volume ($m^3\ mol^{-1}$)

R = Universal gas constant (8.314 $J\ mol^{-1}\ K^{-1}$)

T = Absolute temperature (K)

P_c = Critical Pressure for the component (Pa)

Tc = Critical temperature for the component (K)

ω = Acentric factor for the component

5.3.2. Reactor Model

The primary reactors RXR-1801 and RXR-1802; and a secondary reactor RXR-2801 are modeled as Aspen Plus® RYield reactor. For the present study, the RYield reactor module is the most suitable and, as shown in Table 3.2, was used by three previous investigators. This type of reactor is considered when the reaction stoichiometry or kinetics is unavailable or cannot be used, but the product yield is available. The reaction conversion yield date is presented in given in Appendix A.1.

The Condenser system unit consists of condenser columns CC-1301, CC-1302, and CC-2301, along with the condenser coolers HX-1501, HX-1502, and HX-2301, respectively. The condenser columns are modeled as Aspen Plus® two-phase flash separator and condenser coolers as Aspen Plus® heater. Each condenser

unit is modeled as two condenser columns, CC-1301 and CC-1301A, along with condenser cooler HX-1501. Similarly, CC-1302A and CC-2301A were modeled for the condensers CC-1302 and CC-2301, respectively. This particular approach is used to model a condenser unit instead of a distillation column because the existing process plant employs the bidirectional flow of the reactor outlet to the condenser and heavy wax return from the condenser to the reactor. It is not feasible to model such bidirectional process flow conditions in the distillation column in Aspen Plus®.

5.3.3. Distillation Model

The distillation section comprises two distillation columns that operate under a vacuum. The first distillation column is RC1–4601, and the second distillation column is RC2–4602. Both columns are packed columns that use structured packing. RC1–4601 packing height is 1.9 m (75 in.), and column diameter is 0.254 m (10 in.). RC2–4602 packing height is 1.955 m (77 in), and column diameter is 0.1524 m (6 in.). The packing HETP (Height Equivalent to a Theoretical Plate) for both columns is 0.4 m [69,70]. The number of stages is calculated using equation 3. Therefore, the number of stages for columns RC1–4601 and RC1–4602 is 4.75 (approximately 5) and 4.89 (approximately 5), respectively:

$$\text{Number of stages} = \frac{\text{Height of packing}}{\text{HETP}} \tag{3}$$

Preliminary specifications of distillation columns were estimated using the short-cut distillation column (DSTWU) included in Aspen Plus®. This procedure employs the Winn-Underwood-Gilliland method that provides an initial estimate of the

minimum reflux ratio. Both the columns have a feed inlet at the bottom and require no reboiler.

With the available information (HETP, pressure drop, feed location) and the results of this analysis (reflux ratio), a rigorous calculation and modeling of the distillation columns were performed using the RadFrac module of Aspen Plus®. RadFrac module calculation is based on mass, equilibrium, summation, and heat (MESH) equations. Estimated energy consumption was based on the cooling energy required by the heat exchangers and pump.

5.4. Assumptions

In the present simulation model, the following assumptions were made:

1. The process occurs at a steady-state
2. The pyrolysis reactor is perfectly mixed
3. MPW is completely pyrolyzed
4. The process is isothermal and adiabatic

5.5. Process Simulation Model

An Aspen Plus® simulation flowsheet for the plastic pyrolysis process is shown in Fig. 5.1. The waste plastic is fed at 500 kg/hr to the pyrolysis reactor at 25°C and 1 atm. The pyrolysis reactors (RXR-1801, RXR-1802, and RXR-2801) were modeled using an RYield reactor. The plastic pyrolysis reaction of the three plastics (PP, PE and PS) occurs at 440°C, and 0.998 atm in primary reactors (RXR-1801 and RXR-1802), and products are formed. After the product formation, the pyrolysis vapour proceeds to the condensing unit. The pyrolysis vapour is

allowed to cool down to 400°C in the condenser columns (CC-1301 and CC-1302) and then further to 330°C at pressure 0.994 atm in the condensing coolers (HX-1501 and HX-1502). This allows heavy wax to condense and then separate from pyrolysis vapours and non-condensable gases in CC-1301A and CC-1302A. This heavy wax then proceeds to the secondary reactor (RXR-2801) for further pyrolyzing, and consequently, the pyrolysis vapour is cooled down to 330°C in the condenser (CC-2301, CC-2301A, and HX-2501).

The mixture of non-condensable gases and pyrolysis vapour from the condensers then go to the distillation section for fractionation. The mixture of non-condensable gases and pyrolysis vapour goes to the first distillation column RC-4601, where heavy oil is separated. This column operates under vacuum pressure at 0.985 atm and temperature close to 100°C and 160°C at the top and bottom. The remaining mixture of non-condensable gases and the light oil vapour from the top of RC-4601 go through a further fractionation process in RC-4602. RC-4602 operates under vacuum pressure at 0.97 atm and temperatures close to 20°C and 90°C at the top and bottom. Both RC-4601 and RC-4602 operate at standard operating conditions provided by the process licensers. The light oil is separated from non-condensable gases in this column.

After the RC– 4602, the non-condensable gases under normal conditions such as propane, ethane, methane, etc., are collected in the tank (TK-4603). The tank (TK-4603) is modeled as a two-phase flash separator and operates under a vacuum of 0.96 atm pressure, preventing flammable non-condensable gases from releasing into the atmosphere. These non-condensable gases are first compressed through

a ring compressor (PMP-4105) to a pressure of 1.25 atm and temperature 43°C. The compressor (PMP-4105) is modeled as an isentropic compressor. These highly compressed non-condensable gases are then stored in the tank (TK-4703), which is modeled as a two-phase flash separator.

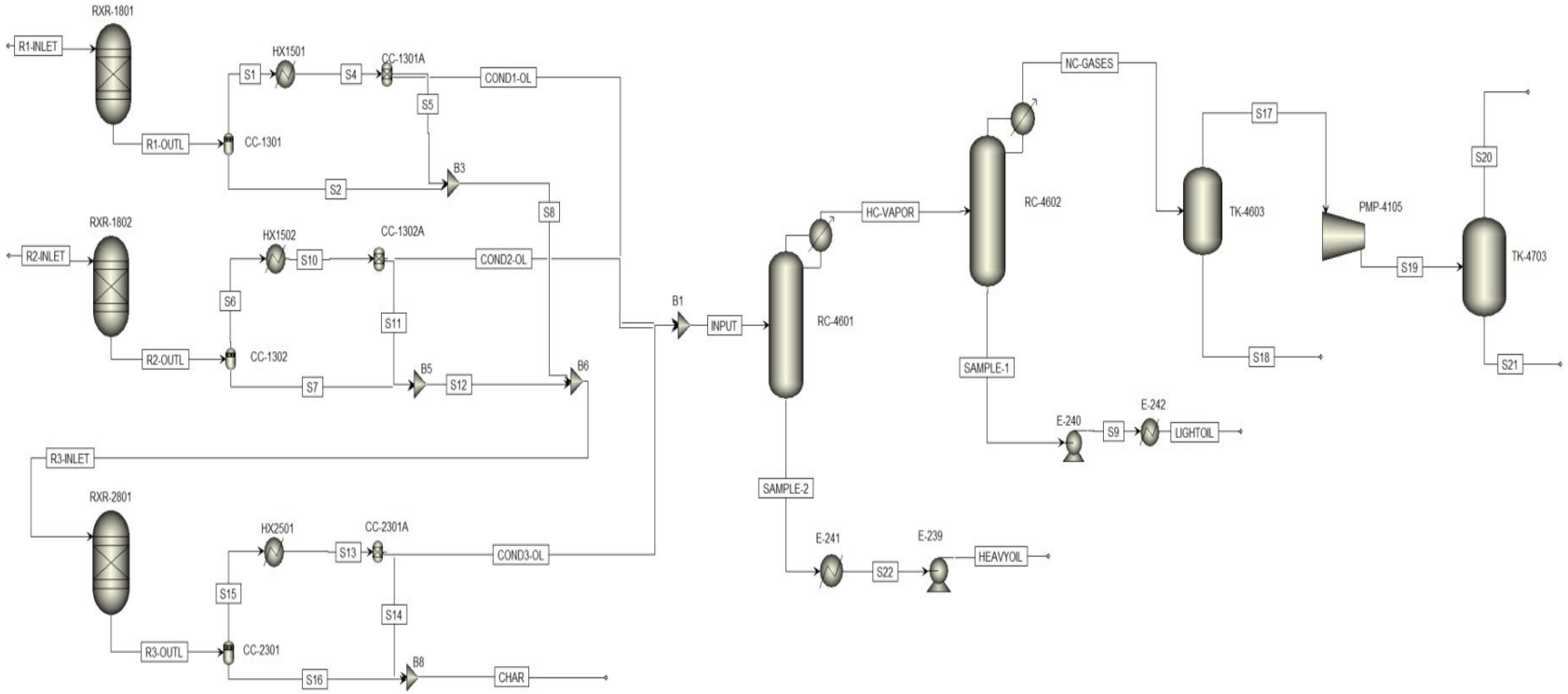

Fig. 5.1: Aspen Plus® simulation flowsheet for the plastic pyrolysis process.

5.6. Sensitivity Analysis

The plastic pyrolysis process produces two liquid products at Sustane: heavy oil and light oil, which has a high economic value. Of the two, light oil is the utmost important product. It holds significant economic value for the plastic pyrolysis process as it nearly resembles naphtha that requires less processing for petrochemical companies to reuse it again to produce plastic and other chemicals. As such, the focus of the technical analysis is on both heavy oil and light oil and two key variables that have the most significant potential impact on the technical performance of the distillation unit and the production of oil fuels.

The two key variables are:

1. The condenser duty of RC-4601
2. The condenser duty of RC-4602

The effects of these two variables on the mass flow rate and physical properties such as density and flash point of heavy oil and light oil are investigated in the sensitivity analysis, and the results are presented in section 6.3.

6. Results And Discussion

In this section, the material and energy balance results of the present simulation study are presented. These results are compared with the experimental data collected at the Sustane Technologies Inc. facility. The comparison of present simulation findings with those reported in the literature is provided. Furthermore, the predictions of the technical sensitivity analysis are discussed in detail.

6.1. Process Simulation Analysis

The plastic pyrolysis process simulation model is presented in Fig 5.2. The results of this simulation obtained at the feed rate of 500 kg/hr, the pyrolysis reactor temperature of 440°C, and the pressure 0.998 atm are presented in this section. Table 6.1 and Table 6.2 summarize the material balance and energy balance.

Table 6.1: Material balance data from simulation

	R1-INLET	R1-OUTL	R2-INLET	R2-OUTL	R3-INLET	R3-OUTL	COND1-OL
Temperature (°C)	25	440	25	440	329.99	440	329.99
Pressure (atm)	1	0.998	1	0.998	0.991	0.998	0.991
Mass Vapour Fraction	0	1	0	1	0	1	1
Mass Flows (kg/hr)	250	250	250	250	54.73	54.73	222.63

	S8	COND2-OL	S12	COND3-OL	CHAR	INPUT	HC-VAPOUR
Temperature (°C)	329.99	329.99	329.99	329.99	329.96	329.99	102.42
Pressure (atm)	0.991	0.991	0.991	0.991	0.991	0.991	0.985
Mass Vapour Fraction	0	1	0	1	0	1	1
Mass Flows (kg/hr)	27.36	222.63	27.36	38.63	16.10	483.89	246.17

	HEAVY OIL	NC-GASES	LIGHT OIL	S17	S19	S20
Temperature (°C)	25	25.20	25	25	43.10	43.10
Pressure (atm)	1	0.97	1	0.96	1.25	1.25
Mass Vapour Fraction	0	1	1	1	1	1
Mass Flows (kg/hr)	237.72	74.26	171.90	74.26	74.26	74.26

Table 6.2: Energy balance data from simulation

	HX-1501	HX-1502	HX-2501	RC-4601	RC-4602	E-239	E-240	E-241
Process Equipment	Cooler	Cooler	Cooler	Distillation Column	Distillation Column	Pump	Pump	Cooler
Utility	Water	Water	Water	Water	Water	Electricity	Electricity	Water
Temperature (°C)	330	330	330	102.42	25.20	25	95.19	25
Heat Duty (kW)	-21.58	-21.58	-4.97	-81.66	-18.55	0.0001	0.0004	-19.41

	E-242	PMP-4105
Process Equipment	Cooler	Compressor
Utility	Water	Electricity
Temperature (°C)	25	43.26
Heat Duty (kW)	-6.95	0.62

The simulation results show an excellent oil yield of 81.92% from the pyrolysis process, whereas the non-condensable gases yield is 14.85%. In comparison with the available literature, the char yield in the present study is reduced to 3.22% as a final product due to the use of a secondary reactor (RXR-2801) that further pyrolyzes the char received from the primary reactors (RXR-1801 and RXR-1802).

6.2. Comparison of Aspen Plus® Predictions with Experimental Data

The light oil and heavy oil densities at 15°C are 759.36 kg/m3 and 837.16 kg/m3, similar to the density obtained from the fuel samples. The flash point for the oil fuels obtained in the simulation is consistent with the samples obtained in the experiments. The following table 6.3 provides the standard density, viscosity, and flash point range for oil fuels:

Table 6.3: Standard physical properties range for oil fuel

Physical Properties	Units	Light oil			Heavy oil		
		Stan.	Exp.	Sim.	Stan.	Exp.	Sim.
Dynamic Viscosity @ 40°C	cP	0.6-0.9	0.62	0.57	1-1.3	1.29	1.08
Density @ 15°C	kg/m^3	750 - 800	768	759	800 - 850	810	837
Flash Point	°C	< 40	< 40	13	> 40	> 40	146

*Stan.: Standard oil properties

*Exp.: Experiment

*Sim.: Simulation

The comparison of Aspen Plus® predictions of light oil and heavy oil with experimental data is presented in Fig. 6.1 and Fig 6.2, respectively. As mentioned in section 5.1, The GC/MS analysis obtained more than 250 components. Therefore, it becomes imperative to consolidate the component list easily and understand the results effectively without diminishing the physical properties of the fuel oils. Hence, the component list for simulation is prepared on the basis of boiling point.

This simulation prediction matches the composition quality of light oil based on a carbon number basis, as shown in Fig. 6.1. It was found that the composition quality of light oil is in good agreement with the GC/MS analysis results.

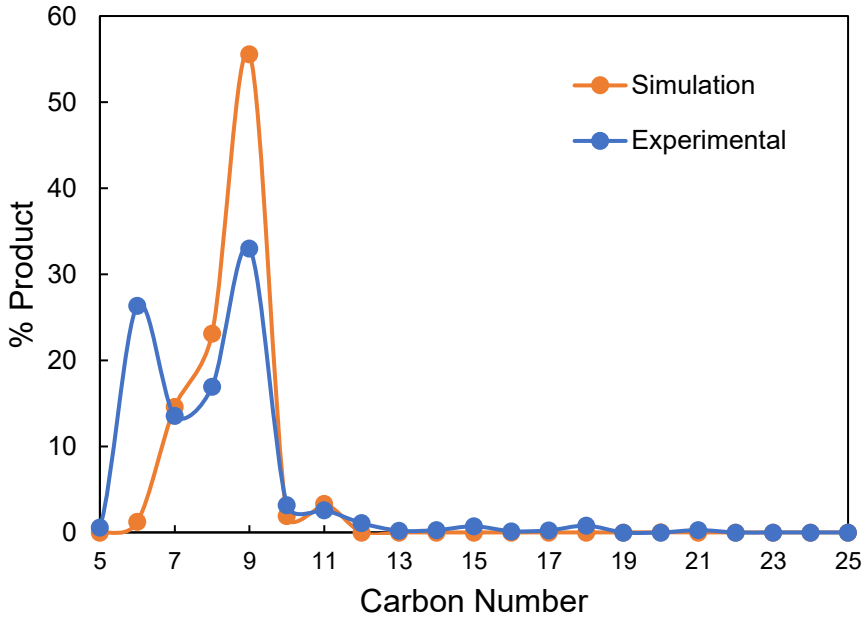

Fig. 6.1: Comparison of Light oil experimental results with predicted results

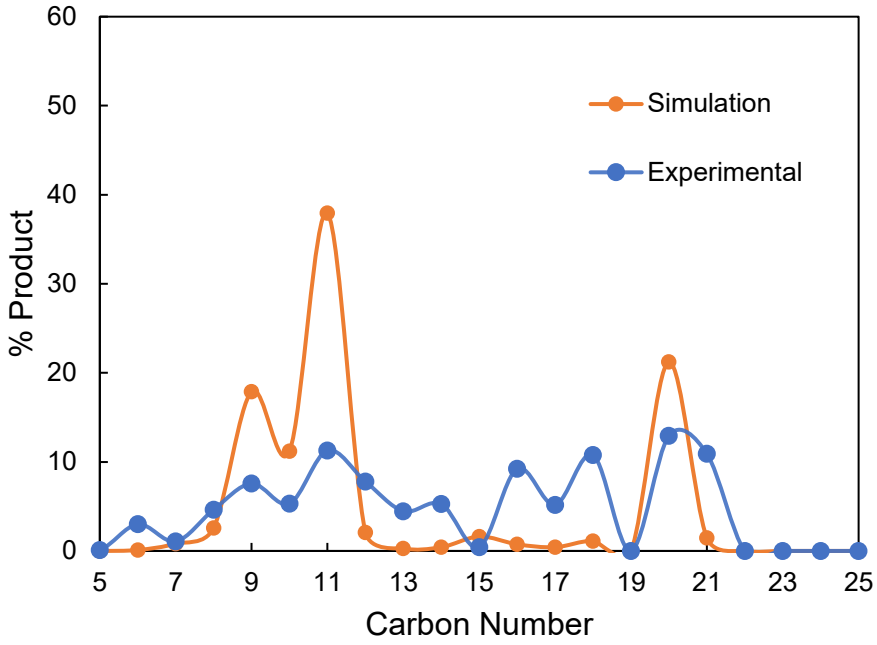

Fig. 6.2: Comparison of Heavy oil experimental results with predicted results

However, the heavy oil results show variance with the results of the GC/MS analysis results, as shown in Fig. 6.2. Bimodal variation is mainly due to the component list. The component list is prepared on the basis of boiling point and not on the basis of carbon number. Many of these components (C_{13}-C_{19}) consist of acetate, alcohol, and alkenes with a significant boiling point range. Therefore, many components from C_{13}-C_{19} had a boiling closer to C_{11}, C_{12} and C_{20}.

6.3. Technical Sensitivity Analysis

In this section, the results of the sensitivity analysis are presented. The effect of the two key variables noted in section 5.4 on the production of heavy oil and light oil is outlined below:

6.3.1. Effect of RC-4601 Condenser Duty

The effect of the RC-4601 condenser duty on the condenser temperature is shown below in Fig. 6.3. In this case, the sensitivity analysis was carried out by changing the condenser duty by more than ± 1.80 kW from its reference condenser duty (i.e., - 81.66 kW). It can be seen from Fig. 6.3 that for the condenser duty range of 5.50 kW, the temperature gradient of only 12.95°C is observed. The maximum achievable condenser temperature is 110.54°C, and the minimum is 98.06°C. The effect of the following temperature and condenser duty on other parameters of heavy oil is discussed below.

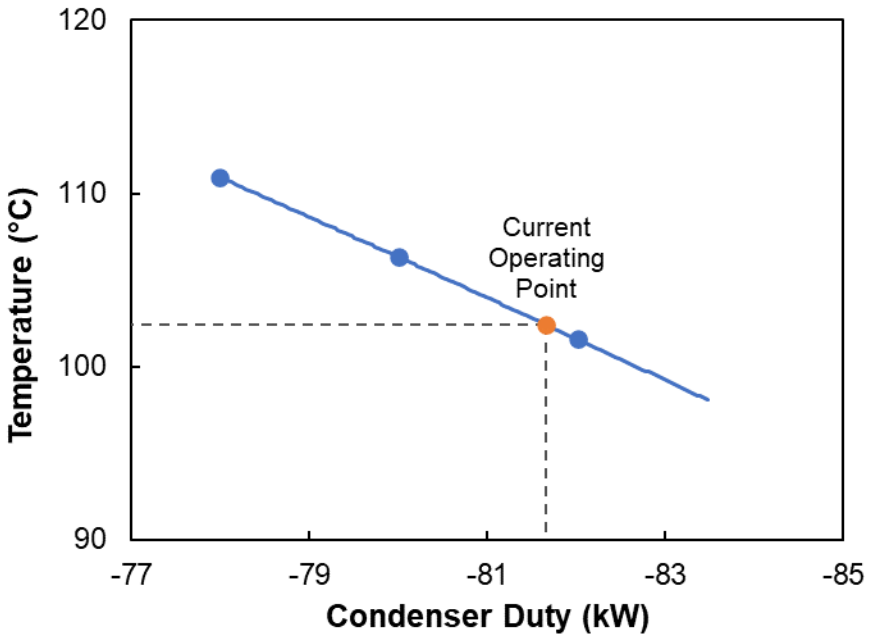

Fig. 6.3: Effect of RC-4601 condenser duty on condenser temperature.

The effect of the RC-4601 condenser duty on the mass flow rate of heavy oil is shown below in Fig. 6.4. The condenser duty is the most sensitive parameter that significantly influences heavy oil production rate and its quality parameters such

as density and flash point. As shown in Fig. 6.4, the production rate of heavy oil increases with the increase in condenser cooling duty and decreases with the decrease in condenser cooling duty.

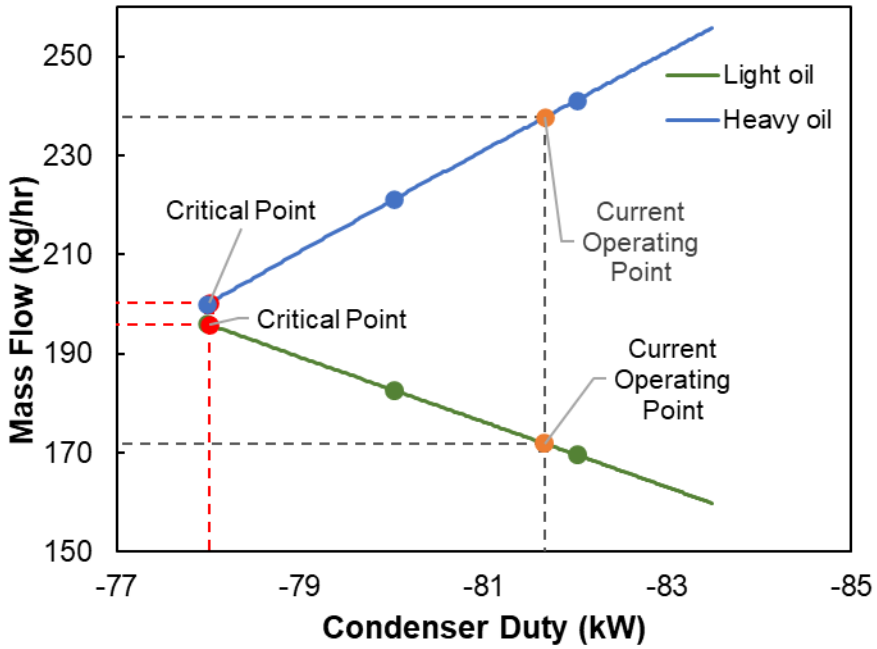

Fig. 6.4: Effect of RC-4601 condenser duty on heavy and light oil production rate.

However, with the increases in condenser cooling duty, the production rate of light oil decreases, as shown in Fig. 6.4. In this case, the RC-4601 condenser duty is varied, and the RC-4602 condenser duty is kept constant at -18.55 kW. The maximum heavy oil production of 255.76 kg/hr can be achieved at condenser duty of – 83.48 kW, increasing more than 7.58% over the predicted heavy oil production. However, the light oil production decreases to 159.83 kg/hr.

The current operating points indicated in the graph are the actual operating points conducted in the simulation. At the critical points, the physical properties of oil fuel exceed the standard specification range provided in table 6.3, which affects the

product quality. At the critical point of -78.16 kW, the density of the heavy oil exceeds the standard density of limit (850 kg/m^3), as shown in Fig. 6.5. Hence operating below such condenser duty affects the product quality, and it is not economically viable.

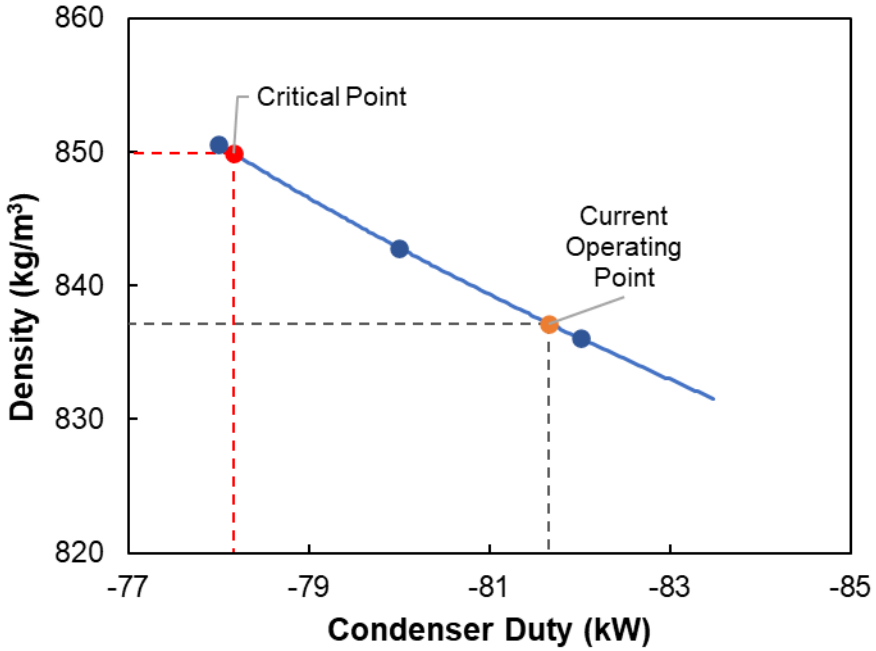

Fig. 6.5: Effect of RC-4601 condenser duty on heavy oil density.

The effect of condenser duty on heavy oil flash point is shown in Fig. 6.6. It shows that the flash point decreases with the increase in condenser cooling duty and increases with the decrease in condenser cooling duty. However, there has not been much change observed in flash point of heavy oil within the operating range of condenser duty.

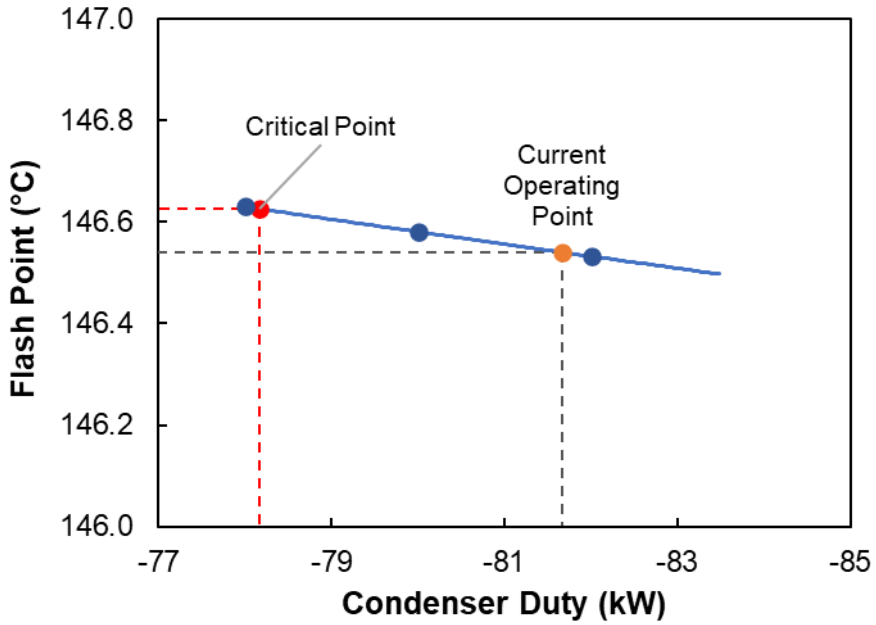

Fig. 6.6: Effect of RC-4601 condenser duty on Flash point of heavy oil.

6.3.2. Effect of RC-4602 Condenser Duty

The effect of the RC-4602 condenser duty on the condenser temperature is shown below in Fig. 6.7. In this case, the sensitivity analysis was carried out by changing the condenser duty by more than ± 2.50 kW from its reference condenser duty (i.e., -18.55 kW). It can be seen from Fig. 6.7 that for the condenser duty range of 16.77 kW, the temperature gradient of 109.29°C is observed. The maximum achievable condenser temperature is 93.80°C, and the minimum is 0°C. At -20.23 kW, the condenser temperature approaches a critical point of 0°C. The effect of the following temperature and condenser duty on other parameters of light oil is discussed below.

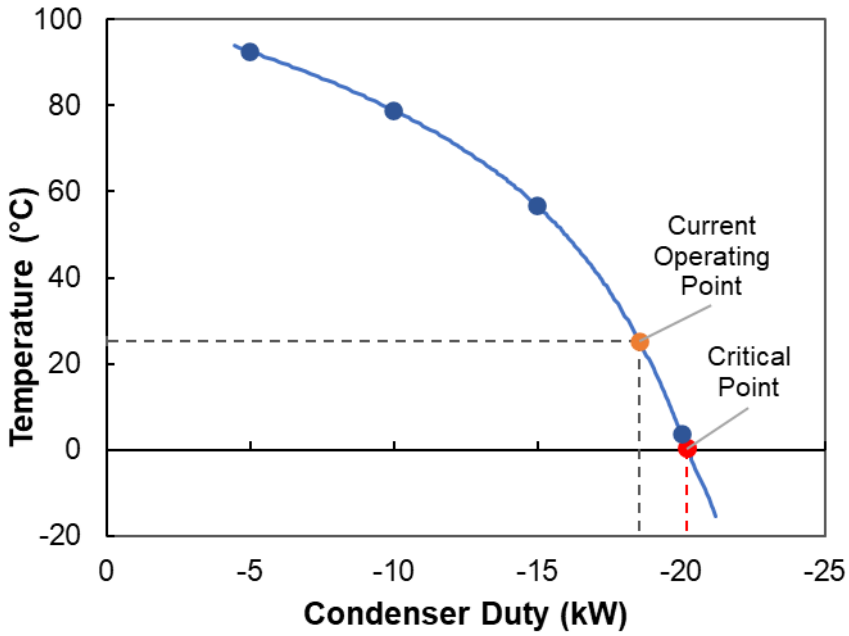

Fig. 6.7: Effect of RC-4602 condenser duty on temperature.

The effect of the RC-4602 condenser duty on the mass flow rate of light oil is shown below in Fig. 6.8. As mentioned above, condenser duty is the most sensitive parameter that significantly influences light oil production rate and its quality parameters such as density and flash point. As shown in Fig. 6.8, the production rate of light oil increases with the increase in condenser cooling duty and decreases with the decrease in condenser cooling duty. The current operating condenser duty is -18.55 kW. The optimum condenser duty obtained is -20.21 kW, where the light oil production rate is 182.07 kg/hr, increasing more than 5.91% over the predicted light oil production rate.

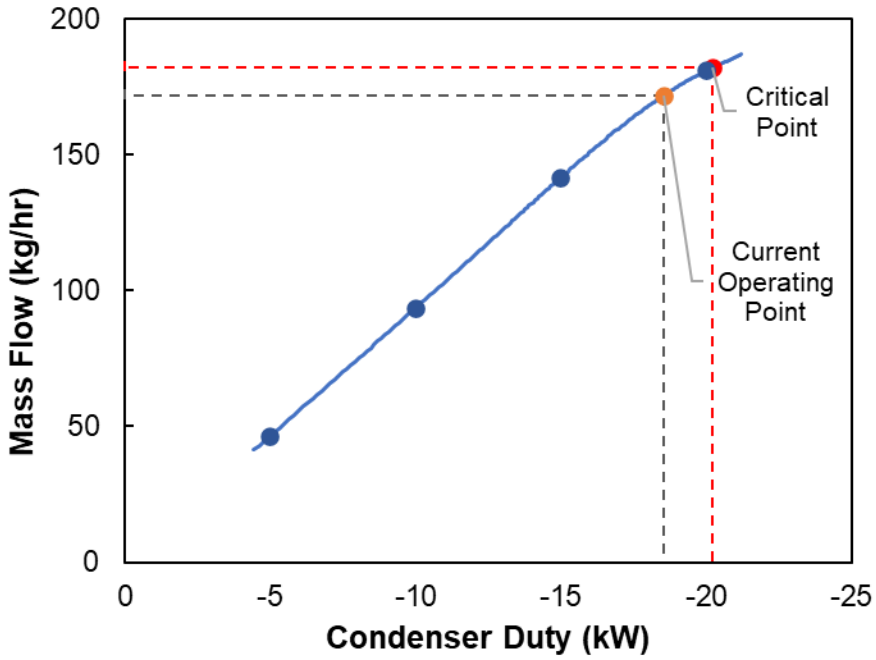

Fig. 6.8: Effect of RC-4602 condenser duty on light oil production rate.

The effect of RC-4602 condenser duty on the density of light oil is shown below in Fig. 6.9. As shown in Fig. 6.9, the density of light oil decreases with the increase in condenser cooling duty and approaches the critical point of -20.23 kW at which the density of the light oil reduced to 756.17 kg/m^3. However, it does not exceed the standard density range of 750-800 kg/m^3.

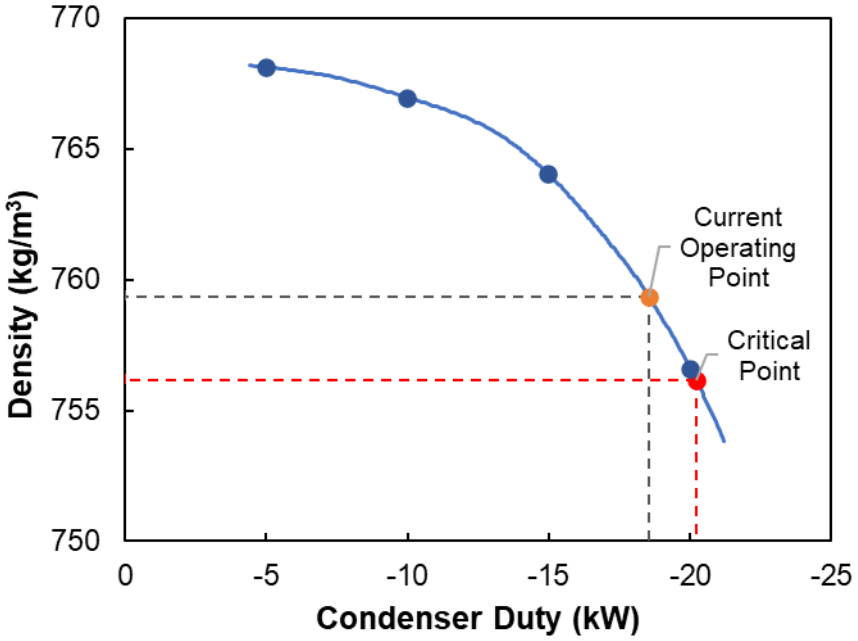

Fig. 6.9: Effect of RC-4602 condenser duty on light oil density.

The effect of RC-4602 condenser duty on light oil flash point is shown in Fig. 6.10. It shows that the flash point decreases with the increase in condenser cooling duty and increases with the decrease in condenser cooling duty. A drop of more than 46% is observed from its maximum with the increase in condenser duty. However, it does not exceed the standard flash point range.

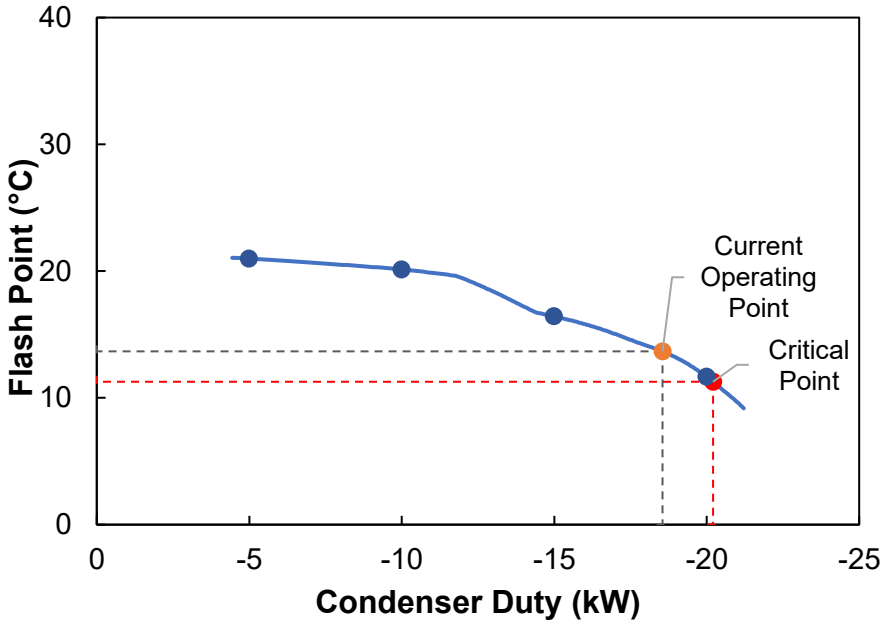

Fig. 6.10: Effect of RC-4602 condenser duty on Flash point of light oil.

6.4. Optimization Analysis

The sensitivity analysis indicates that the condenser duties of distillation columns RC-4601 and RC-4602 significantly impact the production of light and heavy oil. Therefore, an optimization study was performed to find the optimal condenser duty combination that can increase the total oil fuel (a sum of light and heavy oil) production rate and the ratio of light oil to heavy oil, with a particular emphasis on light oil production rate. The optimization study performed for condenser duties was conducted such that the oil fuels did not exceed the critical point of the standard range of physical properties (such as density, flash point and viscosity). The following table 6.4 provides a comparison between optimum column condition and current column operating condition:

Table 6.4: Comparison of optimum column condition and current column operating condition

	Condenser Duty (kW)			Mass Flow Rate (kg/hr)			Light oil/ Heavy oil Ratio
	RC-4601	RC-4602	Total Duty	Light Oil	Heavy Oil	Total Oil	
Optimum condition	-78.21	-23.84	-102.04	217.53	202.29	419.82	1.08
Current condition	-81.66	-18.55	-100.21	171.91	237.73	409.63	0.72

The optimal range of condenser duty for RC-4601 is -78.21 to -78.16 kW and for RC-4602 is -23.84 to -23.85 kW. At the optimum condenser duty of -23.84 kW for RC-4602, the light oil production rate increases to 217.82 kg/hr, an increase of 26.53% over the current operating production rate. The heavy oil production rate decreases at the condenser duty of -78.21 kW for RC-4601. However, with an increase in total condenser duty of 1.82%, the total production rate of oil fuels increases by 2.49% and the light oil to heavy oil production ratio increases from the current operating ratio of 0.72 to 1.08. The optimization data is presented in Appendix A3.

However, there is a limitation to the light oil production rate. As more material is allowed to pass through RC-4601, the increased light oil production rate could lead to RC-4602 column flooding or insufficient condensing capacity in the condenser of RC-4602, resulting in the accumulation of liquid in the downstream knockout drum. The reduced liquid reflux back into RC-4601 may also reduce the heavy oil downflow to a value below the recommended column liquid carrying capacity in RC-4601, creating maldistribution in the column. Prior to proposed optimum

conditions being imposed, the operating limitations in each column need to be confirmed to ensure that the changes in gas/liquid flow capacities and condenser duty can be physically achieved. This optimum was determined for an average reactor outlet composition based on a limited data set of experimental measurements. Recognizing that the fractions of char, heavy oil, light oil and non-condensable will vary over time with different feedstocks, the specific optimization conditions will change. As long as maximizing light oil production is of interest, this work suggests that a control strategy should be adopted which minimizes the condenser duty in RC-4601 by monitoring the density of the heavy oil stream and targeting a value that is as close as possible to the industry accepted limits. This will maximize the flow of potential light oil products through to RC-4602 while still producing a salable product in the heavy oil. The use of an online density meter with temperature-correction factors could be a potential option to achieve this. For RC-4602, the primary quality metric governing operation of the condenser is the flash point of the light oil stream. As more of the lower boiling point compounds are condensed, and exit with the light oil, the vapor pressure and flash point will increase. Routine or online measurement of the flash point of the light oil stream may be a viable control strategy for the operation of the RC-4602 condenser and will likely be required due to the rapid approach towards the flash-point limit of 10°C as the condenser duty is increased.

7. Conclusion And Future Work

7.1. Summary

The present study assessed the distillation unit for Sustane Technologies Inc.'s municipal waste plastic pyrolysis process. An attempt has been made to derive material and energy balances for the plastic pyrolysis process based on a few assumptions related to reactor outlet compositions and a detailed process simulation model using Aspen Plus® version 10. However, the energy balance for the pyrolysis reactors is not included due to the limited information related to reaction kinetics and energy consumption of reactors. In addition, the technical sensitivity analysis and optimization analysis were investigated in the distillation unit.

The process simulation study was conducted for the actual plant capacity of 500 kg/hr of plastic waste, consisting of a mixture of 71.40% polypropylene, 20.40% polyethylene, and 8.20% polystyrene. This plastic mixture is pyrolyzed under the temperature of 440°C and slight vacuum pressure of 0.998 atm to convert it into char, liquid oils, and non-condensable gases. The total oil fuel yield is 81.92%, whereas the non-condensable gases yield is 14.85%. The char yield is reduced to 3.22% due to the use of a secondary reactor that further pyrolyzes the char received from the primary reactors. The light oil and heavy oil fuel densities at 15°C are 759.36 kg/m^3 and 837.16 kg/m^3, similar to the density obtained from the fuel samples from the experimental runs. Also, a flash point for light oil and heavy oil is similar to the fuel samples and consistent with fuel standards.

The yield of heavy oil is 237.72 kg/hr, and light oil is 171.90 kg/hr. Light oil holds higher economic value than heavy oil as it nearly resembles naphtha that requires less processing for petrochemical companies to reuse it again to produce plastic and other chemicals.

Furthermore, a technical sensitivity analysis for liquid oils was performed across the columns RC-4601 and RC-4602 with two key variables: RC-4601 condenser duty and RC-4602 condenser duty. The condenser duty is the most sensitive parameter that significantly influences light oil and heavy oil production rate and its quality parameters such as density and flash point.

The technical analysis shows that the maximum achievable condenser temperature of the column RC-4601 is 110.54°C, and the minimum is 98.06°C. The production rate of heavy oil increases with the increase in condenser cooling duty and decreases with the decrease in condenser cooling duty. The maximum heavy oil production of 255.76 kg/hr can be achieved at condenser duty of – 83.48 kW. However, the light oil production decreases to 159.83 kg/hr. At the critical point of -78.16 kW, the density of the heavy oil exceeds the standard density of limit (850 kg/m^3). However, variations in RC-4601 condenser duty have shown no effect on the flash point of heavy oil.

Similarly, for the column RC-4602, the maximum achievable condenser temperature is 93.80°C, and the minimum is 0°C. At -20.23 kW, the condenser temperature approaches a critical point of 0°C. The production rate of light oil increases with the increase in condenser cooling duty and decreases with the decrease in condenser cooling duty. The optimum condenser duty obtained is -

20.21 kW, where the light oil production rate is 182.07 kg/hr, increasing more than 5.91% over the predicted light oil production rate. At the critical point of -20.23 kW, the density of the light oil reduced to 756.17 kg/m^3. However, it does not exceed the standard density range of 750-800 kg/m^3. The flash point of light oil decreases with the increase in condenser cooling duty and increases with the decrease in condenser cooling duty. A drop of more than 46% is observed from its maximum with the increase in condenser duty. However, it does not exceed the standard flash point range.

Additionally, an optimization study was performed to find the optimal condenser duties combination that can increase the total oil fuel (a sum of light and heavy oil) production rate and the ratio of light oil to heavy oil, with a particular emphasis on light oil production rate. The optimal range of condenser duty for RC-4601 is -78.21 to -78.16 kW and for RC-4602 is -23.84 to -23.85 kW. At the optimum condenser duty of -23.84 kW for RC-4602, the light oil production rate increases to 217.82 kg/hr, an increase of 26.53% over the current operating production rate. The heavy oil production rate decreases at the condenser duty of -78.21 kW for RC-4601. However, with an increase in total condenser duty of 1.82%, the total production rate of oil fuels increases by 2.49% and the light oil to heavy oil production ratio increases from the current operating ratio of 0.72 to 1.08.

References

[1] L. Lebreton, A. Andrady, Future scenarios of global plastic waste generation and disposal, Palgrave Commun. 5 (2019) 1–11. https://doi.org/10.1057/s41599-018-0212-7.

[2] E. and C.C. Canada, Canada one-step closer to zero plastic waste by 2030, (n.d.). https://www.canada.ca/en/environment-climate-change/news/2020/10/canada-one-step-closer-to-zero-plastic-waste-by-2030.html.

[3] G. Gourmelon, Global Plastic Production Rises, Recycling Lags | Worldwatch Institute, WorldWatch Inst. (2015) 1–7.

[4] M. Eriksen, L.C.M. Lebreton, H.S. Carson, M. Thiel, C.J. Moore, J.C. Borerro, F. Galgani, P.G. Ryan, J. Reisser, Plastic Pollution in the World's Oceans: More than 5 Trillion Plastic Pieces Weighing over 250,000 Tons Afloat at Sea, PLoS One. 9 (2014) 1–15. https://doi.org/10.1371/journal.pone.0111913.

[5] R. Ward, Nova Scotia only reaches 20 per cent of waste diversion target, CBC News. (2016). https://www.cbc.ca/news/canada/nova-scotia/waste-diversion-target-missed-1.3309123.

[6] A.K. Panda, R.K. Singh, D.K. Mishra, Thermolysis of waste plastics to liquid fuel. A suitable method for plastic waste management and manufacture of value added products-A world prospective, Renew. Sustain. Energy Rev. 14 (2010) 233–248. https://doi.org/10.1016/j.rser.2009.07.005.

[7] M. of E. Canada, Regulation Amending the Sulphur in Gasoline Regulations: SOR/2020-277, Canada Gazette, Part II. (n.d.) 26. https://gazette.gc.ca/rp-pr/p2/2020/2020-12-23/html/sor-dors277-eng.html.

[8] CCME, Strategy on Zero Plastic Waste, Can. Counc. Minist. Environ. (2018) 14. https://www.ccme.ca/files/Resources/waste/plastics/STRATEGY ON ZERO PLASTIC WASTE.pdf.

[9] J.R. Banu, V.G. Sharmila, U. Ushani, V. Amudha, G. Kumar, Impervious and influence in the liquid fuel production from municipal plastic waste through thermo-chemical biomass conversion technologies - A review, Sci. Total Environ. 718 (2020). https://doi.org/10.1016/j.scitotenv.2020.137287.

[10] S.M. Al-Salem, A. Antelava, A. Constantinou, G. Manos, A. Dutta, A review on thermal and catalytic pyrolysis of plastic solid waste (PSW), J. Environ. Manage. 197 (2017) 177–198. https://doi.org/10.1016/j.jenvman.2017.03.084.

[11] P. Kasar, D.K. Sharma, M. Ahmaruzzaman, Thermal and catalytic decomposition of waste plastics and its co-processing with petroleum residue through pyrolysis process, J. Clean. Prod. 265 (2020) 121639. https://doi.org/10.1016/j.jclepro.2020.121639.

[12] F. Zhang, Y. Zhao, D. Wang, M. Yan, J. Zhang, P. Zhang, T. Ding, L. Chen, C. Chen, Current technologies for plastic waste treatment : A review, J. Clean. Prod. (2020) 124523. https://doi.org/10.1016/j.jclepro.2020.124523.

[13] G. Evans, C. Smith, Biomass to liquids technology, Elsevier Ltd., 2012. https://doi.org/10.1016/B978-0-08-087872-0.00515-1.

[14] C. Wu, X. Tu, Biological and fermentative conversion of syngas, Handb. Biofuels Prod. Process. Technol. Second Ed. (2016) 335–357. https://doi.org/10.1016/B978-0-08-100455-5.00012-6.

[15] J.J. Orgill, H.K. Atiyeh, M. Devarapalli, J.R. Phillips, R.S. Lewis, R.L. Huhnke, A comparison of mass transfer coefficients between trickle-bed, Hollow fiber membrane and stirred tank reactors, Bioresour. Technol. 133 (2013) 340–346. https://doi.org/10.1016/j.biortech.2013.01.124.

[16] J.R. Phillips, R.L. Huhnke, H.K. Atiyeh, Syngas fermentation: A microbial conversion process of gaseous substrates to various products, Fermentation. 3 (2017). https://doi.org/10.3390/fermentation3020028.

[17] A. Kapic, S.T. Jones, T.J. Heindel, Carbon monoxide mass transfer in a syngas mixture, Ind. Eng. Chem. Res. 45 (2006) 9150–9155. https://doi.org/10.1021/ie060655u.

[18] R. Miandad, M. Rehan, M.A. Barakat, A.S. Aburiazaiza, H. Khan, I.M.I. Ismail, J. Dhavamani, J. Gardy, A. Hassanpour, A.S. Nizami, Catalytic pyrolysis of plastic waste: Moving toward pyrolysis based biorefineries, Front. Energy Res. 7 (2019) 1–17. https://doi.org/10.3389/fenrg.2019.00027.

[19] S.D. Anuar Sharuddin, F. Abnisa, W.M.A. Wan Daud, M.K. Aroua, A review on pyrolysis of plastic wastes, Energy Convers. Manag. 115 (2016) 308–326. https://doi.org/10.1016/j.enconman.2016.02.037.

[20] K. Moorthy Rajendran, V. Chintala, A. Sharma, S. Pal, J.K. Pandey, P. Ghodke, Review of catalyst materials in achieving the liquid hydrocarbon fuels from municipal mixed plastic waste (MMPW), Mater. Today Commun. 24 (2020) 100982. https://doi.org/10.1016/j.mtcomm.2020.100982.

[21] A. Demirbas, Pyrolysis of municipal plastic wastes for recovery of gasoline-range hydrocarbons, J. Anal. Appl. Pyrolysis. 72 (2004) 97–102. https://doi.org/10.1016/j.jaap.2004.03.001.

[22] A.T. Sipra, N. Gao, H. Sarwar, Municipal solid waste (MSW) pyrolysis for bio-fuel production: A review of effects of MSW components and catalysts, Fuel Process. Technol. 175 (2018) 131–147. https://doi.org/10.1016/j.fuproc.2018.02.012.

[23] T. Faravelli, Thermal Degradation of Polystyrene, Anal. Appl. Pyrolysis. 60 (2001) 103–121. https://doi.org/10.1246/nikkashi.1975.1241.

[24] A.G. Buekens, H. Huang, Catalytic plastics cracking for recovery of gasoline-range hydrocarbons from municipal plastic wastes, Resour. Conserv. Recycl. 23 (1998) 163–181. https://doi.org/10.1016/S0921-3449(98)00025-1.

[25] F. Abnisa, W.M.A. Wan Daud, A review on co-pyrolysis of biomass: An optional technique to obtain a high-grade pyrolysis oil, Energy Convers. Manag. 87 (2014) 71–85. https://doi.org/10.1016/j.enconman.2014.07.007.

[26] R. Miandad, M.A. Barakat, A.S. Aburiazaiza, M. Rehan, I.M.I. Ismail, A.S. Nizami, Effect of plastic waste types on pyrolysis liquid oil, Int. Biodeterior. Biodegrad. 119 (2017) 239–252. https://doi.org/10.1016/j.ibiod.2016.09.017.

[27] M.S. Abbas-Abadi, M.N. Haghighi, H. Yeganeh, A.G. McDonald, Evaluation of pyrolysis process parameters on polypropylene degradation products, J. Anal. Appl. Pyrolysis. 109 (2014) 272–277. https://doi.org/10.1016/j.jaap.2014.05.023.

[28] C. Vasile, M. Brebu, R. Darie, H. Darie, M.A. Uddin, Y. Sakata, Thermal and catalytic decomposition of mixed plastics. III1 PVC-containing mixed plastics, Rev. Roum. Chim. 47 (2002) 1185–1191.

[29] Y. Uemichi, J. Nakamura, T. Itoh, M. Sugioka, A.A. Garforth, J. Dwyer, Conversion of polyethylene into gasoline-range fuels by two-stage catalytic degradation using silica-alumina and HZSM-5 zeolite, Ind. Eng. Chem. Res. 38 (1999) 385–390. https://doi.org/10.1021/ie980341+.

[30] P. Onu, C. Vasile, S. Ciocîlteu, E. Iojoiu, H. Darie, Thermal and catalytic decomposition of polyethylene and polypropylene, J. Anal. Appl. Pyrolysis. 49 (1999) 145–153. https://doi.org/10.1016/S0165-2370(98)00109-0.

[31] U. Arena, M.L. Mastellone, Fluidized Bed Pyrolysis of Plastic Wastes, 2006. https://doi.org/10.1002/0470021543.ch16.

[32] W. Kaminsky, M. Predel, A. Sadiki, Feedstock recycling of polymers by pyrolysis in a fluidised bed, Polym. Degrad. Stab. 85 (2004) 1045–1050. https://doi.org/10.1016/j.polymdegradstab.2003.05.002.

[33] P.T. Williams, E.A. Williams, Fluidised bed pyrolysis of low density polyethylene to produce petrochemical feedstock, J. Anal. Appl. Pyrolysis. 51 (1999) 107–126. https://doi.org/10.1016/S0165-2370(99)00011-X.

[34] M.P. Systems, Pyrolysis penetrates power from waste market, (1998). https://www.modernpowersystems.com/features/featurepyrolysis-penetrates-power-from-waste-market/.

[35] Y. Zhang, G. Ji, D. Ma, C. Chen, Y. Wang, W. Wang, A. Li, Liquid oils produced from pyrolysis of plastic wastes with heat carrier in rotary kiln, Process Saf. Environ. Prot. 142 (2020) 203–211. https://doi.org/10.1016/j.psep.2020.06.021.

[36] A.D. Russell, E.I. Antreou, S.S. Lam, C. Ludlow-Palafox, H.A. Chase, Microwave-assisted pyrolysis of HDPE using an activated carbon bed, RSC Adv. 2 (2012) 6756–6760. https://doi.org/10.1039/c2ra20859h.

[37] A. Undri, L. Rosi, M. Frediani, P. Frediani, Efficient disposal of waste polyolefins through microwave assisted pyrolysis, Fuel. 116 (2014) 662–671. https://doi.org/10.1016/j.fuel.2013.08.037.

[38] A.A. Sobko, Generalized van der Waals-Berthelot equation of state, Dokl. Phys. 53 (2008) 416–419. https://doi.org/10.1134/S1028335808080028.

[39] C.J.M. Lasance, The thermal conductivity of unfilled plastics, Electron. Cool. (2001).

[40] L.W. McKeen, Effect of Radiation on the Properties of Polyester Polymers, 2020. https://doi.org/10.1016/b978-0-12-819729-5.00004-9.

[41] M. Sarker, A. Kabir, M.M. Rashid, M. Molla, A.S.M. Din Mohammad, Waste Polyethylene Terephthalate (PETE-1) Conversion into Liquid Fuel, J. Fundam. Renew. Energy Appl. 1 (2011) 1–5. https://doi.org/10.4303/jfrea/r101202.

[42] O. Cepeliogullar, A. E. Putun, Utilization of Two Different Types of Plastic Wastes from Daily and Industrial Life, J. Selcuk Univ. Nat. Appl. Sci. (2000) 694–706. http://citeseerx.ist.psu.edu/viewdoc/download?doi=10.1.1.868.1453&rep=rep1&type=pdf%0Ahttp://josunas.selcuk.edu.tr/login/index.php/josunas/article/view/200.

[43] Omnexus, Polyethylene (PE) - Complete Guide, (n.d.). https://omnexus.specialchem.com/selection-guide/polyethylene-plastic.

[44] J.M. Sustaita-Rodríguez, F.J. Medellín-Rodríguez, D.C. Olvera-Mendez, A.J. Gimenez, G. Luna-Barcenas, Thermal Stability and Early Degradation Mechanisms of High-Density Polyethylene, Polyamide 6 (Nylon 6), and Polyethylene Terephthalate, Polym. Eng. Sci. 59 (2019) 2016–2023. https://doi.org/10.1002/pen.25201.

[45] B.L.F. Chin, S. Yusup, A. Al Shoaibi, P. Kannan, C. Srinivasakannan, S.A. Sulaiman, Kinetic studies of co-pyrolysis of rubber seed shell with high density polyethylene, Energy Convers. Manag. 87 (2014) 746–753. https://doi.org/10.1016/j.enconman.2014.07.043.

[46] I. Dubdub, M. Al-Yaari, Pyrolysis of low density polyethylene: Kinetic study using TGA data and ANN prediction, Polymers (Basel). 12 (2020). https://doi.org/10.3390/POLYM12040891.

[47] A. Marcilla, M.I. Beltrán, R. Navarro, Evolution of products during the degradation of polyethylene in a batch reactor, J. Anal. Appl. Pyrolysis. 86 (2009) 14–21. https://doi.org/10.1016/j.jaap.2009.03.004.

[48] Q. Wu, S. Chen, H. Liu, Effect of surface chemistry of polyethyleneimine-grafted polypropylene fiber on its CO2 adsorption, RSC Adv. 4 (2014) 27176–27183. https://doi.org/10.1039/c4ra01232a.

[49] D.K. Mandal, H. Bhunia, P.K. Bajpai, V.K. Bhalla, Thermal degradation kinetics and estimation of lifetime of radiation grafted polypropylene films, Radiat. Phys. Chem. 136 (2017) 1–8. https://doi.org/10.1016/j.radphyschem.2017.03.036.

[50] S.H. Jung, M.H. Cho, B.S. Kang, J.S. Kim, Pyrolysis of a fraction of waste polypropylene and polyethylene for the recovery of BTX aromatics using a fluidized bed reactor, Fuel Process. Technol. 91 (2010) 277–284. https://doi.org/10.1016/j.fuproc.2009.10.009.

[51] M.S. Abbas-Abadi, K.M. Van Geem, M. Fathi, H. Bazgir, M. Ghadiri, The pyrolysis of oak with polyethylene, polypropylene and polystyrene using fixed bed and stirred reactors and TGA instrument, Energy. 232 (2021) 121085. https://doi.org/10.1016/j.energy.2021.121085.

[52] L. Ding, J. Zhao, Y. Pan, J. Guan, J. Jiang, Q. Wang, Insights into Pyrolysis of Nano-Polystyrene Particles: Thermochemical Behaviors and Kinetics Analysis, J. Therm. Sci. 28 (2019) 763–771. https://doi.org/10.1007/s11630-019-1123-7.

[53] F.J. Mastral, E. Esperanza, P. Garciía, M. Juste, Pyrolysis of high-density polyethylene in a fluidised bed reactor. Influence of the temperature and residence time, J. Anal. Appl. Pyrolysis. 63 (2002) 1–15. https://doi.org/10.1016/S0165-2370(01)00137-1.

[54] J.A. Onwudili, N. Insura, P.T. Williams, Composition of products from the pyrolysis of polyethylene and polystyrene in a closed batch reactor: Effects of temperature and residence time, J. Anal. Appl. Pyrolysis. 86 (2009) 293–303. https://doi.org/10.1016/j.jaap.2009.07.008.

[55] K. Murata, K. Sato, Y. Sakata, Effect of pressure on thermal degradation of polyethylene, J. Anal. Appl. Pyrolysis. 71 (2004) 569–589. https://doi.org/10.1016/j.jaap.2003.08.010.

[56] J.N. Sahu, K.K. Mahalik, H.K. Nam, T.Y. L, Feasibility study for catalytic cracking of waste plastic to produce fuel oil with reference to Malaysia and simulation using ASPEN Plus, Environ. Prog. Sustain. Energy. 33 (2014) 676–680. https://doi.org/10.1002/ep.

[57] S.O.A.A. Mohamed Magzoub Garieb Alla*, SIMULATION AND DESIGN FOR PROCESS TO CONVERT PLASTIC WASTE TO LIQUID FUEL USING ASPEN HYSYS PROGRAM, Integr. J. Eng. Res. Technol. Content. 1 (2015) 270–274.

[58] N.-O. Ekpe Moses, Modelling and Simulation of Waste Plastic Power Plant: A Theoretical Framework, Am. J. Chem. Eng. 6 (2018) 94. https://doi.org/10.11648/j.ajche.20180605.13.

[59] A.G. Adeniyi, O.A.A. Eletta, J.O. Ighalo, Computer aided modelling of low density polyethylene pyrolysis to produce synthetic fuels, Niger. J. Technol. 37 (2018) 945. https://doi.org/10.4314/njt.v37i4.12.

[60] A. Fivga, I. Dimitriou, Pyrolysis of plastic waste for production of heavy fuel substitute: A techno-economic assessment, Energy. 149 (2018) 865–874. https://doi.org/10.1016/j.energy.2018.02.094.

[61] N. Deng, D. Li, Q. Zhang, A. Zhang, R. Cai, B. Zhang, Simulation analysis of municipal solid waste pyrolysis and gasification based on Aspen plus, Front. Energy. 13 (2019) 64–70. https://doi.org/10.1007/s11708-017-0481-7.

[62] G. Jiang, J. Wang, S.M. Al-Salem, G.A. Leeke, Molten Solar Salt Pyrolysis of Mixed Plastic Waste: Process Simulation and Technoeconomic Evaluation, Energy and Fuels. 34 (2020) 7397–7409. https://doi.org/10.1021/acs.energyfuels.0c01052.

[63] T. Selvaganapathy, R. Muthuvelayudham, J.K. M, Steady State Simulation of Plastic Pyrolysis Process using Aspen Hysys V9 Simulator, Int. J. Recent Technol. Eng. 8 (2019) 2206–2211. https://doi.org/10.35940/ijrte.d7885.118419.

[64] M. Lameh, A. Abbas, F. Azizi, J. Zeaiter, A simulation-based analysis for the performance of thermal solar energy for pyrolysis applications, Int. J. Energy Res. 45 (2021) 15022–15035. https://doi.org/10.1002/er.6781.

[65] R.M. and M.J.K. T. Selvaganapathy1*, Simulation of Waste Plastic Pyrolysis Process Using Aspen Hysys V9 Simulator under Steady State Operating Condition, Emerg. Trends Eng. Res. Technol. Vol. 2. (2020). https://doi.org/10.9734/bpi/etert/v2.

[66] S. Luo, Research on Municipal Solid Waste Shredder and Effect of Particle Size on Pyrolysis & Gasification Performance, Huazhong University of Science and Technology, 2010. https://m.dissertationtopic.net/doc/1544499.

[67] S.E. Levine, L.J. Broadbelt, Detailed mechanistic modeling of high-density polyethylene pyrolysis: Low molecular weight product evolution, Polym. Degrad. Stab. 94 (2009) 810–822. https://doi.org/10.1016/j.polymdegradstab.2009.01.031.

[68] International Energy Agency, Composition of gasoline and diesel, Int. Energy Agency - Adv. Mot. Fuels. (n.d.). https://www.iea-amf.org/content/fuel_information/diesel_gasoline#:~:text=Diesel fuel consists mainly of,170 and 360 °C.

[69] F.H. Yin, C.G. Sun, A. Afacan, K. Nandakumar, K.T. Chuang, CFD modeling of mass-transfer processes in randomly packed distillation columns, Ind. Eng. Chem. Res. 39 (2000) 1369–1380. https://doi.org/10.1021/ie990539+.

[70] J.S. Eckert, Selecting the proper distillation column packing, Chem Eng Progr. (1970). https://ceng.tu.edu.iq/ched/images/lectures/chem-lec/st4/c1/EQUIPMENT_DESIGN_LECTURE_25 mass transfer equipment 3.pdf.

Appendices

A.1: Component Yield Data

Component	Chemical Formula	Conversion Yield (%)
Methane	CH_4	3.62%
Ethane	C_2H_6	1.08%
ethylene	C_2H_4	2.83%
Propane	C_3H_8	0.20%
Propylene	C_3H_6	1.87%
Methylpropane	C_4H_{10}	0.03%
butane	C_4H_{10}	0.03%
acetylene	C_2H_2	0.03%
trans2butene	C_4H_8	0.00%
1butene	C_4H_8	0.10%
isobutylene	C_4H_8	0.17%
n-Hexane	C_6H_{14}	2.18%
2,4-Dimethyl-1-heptene	C_9H_{18}	9.66%
1,3,5-Cycloheptatriene	C_7H_8	3.13%
2-Pentanone,3-[(acetyloxy)methyl]-3,4-dimethyl-, (+-.)-	$C_{10}H_{18}O_3$	8.15%
Heptane, 4-methyl-	C_8H_{18}	1.71%
Ethylbenzene	C_8H_{10}	1.30%
Cyclohexane, 1,3,5-trimethyl-	C_9H_{18}	3.37%
1-Heptene	C_7H_{14}	1.78%

Component	Chemical Formula	Conversion Yield (%)
Styrene	C_8H_8	1.96%
Cyclopropane, 1-heptyl-2-methyl-	$C_{11}H_{22}$	5.97%
2-Isopropyl-5-methyl-1-heptanol	$C_{11}H_{24}O$	1.35%
Nonane, 2,6-dimethyl-	$C_{11}H_{24}$	6.23%
1-Nonene	C_9H_{18}	1.80%
1-Octene	C_8H_{16}	0.72%
Octane	C_8H_{18}	0.53%
Decane	$C_{10}H_{22}$	4.96%
Nonane	C_9H_{20}	5.18%
1-Heptene, 2-methyl-	C_8H_{16}	1.59%
Dodecane	$C_{12}H_{26}$	0.61%
Nonane, 2-methyl-3-methylene-	$C_{11}H_{22}$	4.87%
Heptadecane, 2,6,10,14-tetramethyl-	$C_{21}H_{44}$	0.65%
Cyclohexene, 3,3,5-trimethyl-	C_9H_{16}	1.49%
(2,4,6-Trimethylcyclohexyl) methanol	$C_{10}H_{20}O$	0.80%
Cyclohexene, 3-methyl-	C_7H_{12}	1.15%
Cyclopentane, 1,1,3,4-tetramethyl-, cis-	C_9H_{18}	0.52%
1-Dodecanol, 3,7,11-trimethyl-	$C_{15}H_{32}O$	0.70%
Benzene, 1-ethyl-3-methyl-	C_9H_{12}	4.84%

Component	Chemical Formula	Conversion Yield (%)
Benzene, 1,3-dimethyl- (M-Xylene)	C_8H_{10}	0.28%
Benzene, 1,2,4-trimethyl-	C_9H_{12}	0.07%
1H-Indene, 3-methyl-	$C_{10}H_{10}$	0.06%
1H-Indene, 1-methylene-	$C_{10}H_8$	0.02%
2-Decene, 7-methyl-, (Z)-	$C_{11}H_{22}$	0.07%
Naphthalene, 1-methyl-	$C_{11}H_{10}$	0.04%
(1-Methylenebut-2-enyl) benzene	$C_{11}H_{12}$	0.02%
Tetra-hydrogeranyl formate	$C_{11}H_{22}O_2$	0.03%
2-Dodecene, (E)-	$C_{12}H_{24}$	0.12%
Naphthalene, 1,7-dimethyl-	$C_{12}H_{12}$	0.01%
2-Tridecene, (E)-	$C_{13}H_{26}$	0.04%
1,12-Tridecadiene	$C_{13}H_{24}$	0.02%
Decane, 2,3,5,8-tetramethyl-	$C_{14}H_{30}$	0.08%
(2R,3R,4aR,5S,8aS)-2-Hydroxy-4a,5-dimethyl-3-(prop-1-en-2-yl)oct	$C_{15}H_{24}O_2$	0.00%
7-Hexadecene, (Z)-	$C_{16}H_{32}$	0.11%
1-Hexadecanol	$C_{16}H_{34}O$	0.04%
1-Hexadecanol, 2-methyl-	$C_{17}H_{36}O$	0.08%
Hexadecane, 1-(ethenyloxy)-	$C_{18}H_{36}O$	0.12%
11,13-Dimethyl-12-tetradecen-1-ol acetate	$C_{18}H_{34}O_2$	0.10%
5-Eicosene, (E)-	$C_{20}H_{40}$	0.07%
Ethanol, 2-(octadecyloxy)-	$C_{20}H_{42}O_2$	0.52%

Component	Chemical Formula	Conversion Yield (%)
7-Octadecyne, 2-methyl-	$C_{19}H_{36}$	0.41%
P-terphenyl	$C_{18}H_{14}$	0.42%
M-terphenyl	$C_{18}H_{14}$	0.45%
Benzyl-butyl-phthalate	$C_{19}H_{20}O_4$	0.48%
1-3-5 triphenyl benzene	$C_{24}H_{18}$	1.09%
3-3-diphenylbenzene	$C_{24}H_{18}$	1.06%
n-Pentacosane	$C_{25}H_{52}$	1.08%
1-hexacosene	$C_{26}H_{52}$	1.14%
n-hexacosane	$C_{26}H_{54}$	1.12%
1-heptacosene	$C_{27}H_{54}$	1.10%
n-heptacosane	$C_{27}H_{56}$	1.00%
1-octacosene	$C_{28}H_{56}$	0.86%
n-octacosane	$C_{28}H_{58}$	0.74%
Total		100.00%

A.2: Data from Sensitivity Analysis Results

B.1: Effect of RC-4601 condenser duty on various parameters

RC-4601 Condenser Duty (kW)	HC-Vapor Temp. (°C)	Heavy Oil Mass Flow (kg/hr)	Heavy Oil Density (kg/m^3)	Heavy Oil Flash Point (°C)
-78.00	110.91	200.07	850.59	146.63
-78.12	110.63	201.41	850.06	146.63
-78.21	110.44	202.29	849.72	146.62
-78.25	110.35	202.73	849.54	146.62
-78.29	110.26	203.16	849.37	146.62
-78.41	109.98	204.47	848.87	146.62
-78.49	109.79	205.33	848.54	146.62
-78.62	109.52	206.60	848.05	146.61
-78.70	109.33	207.45	847.73	146.61
-78.82	109.06	208.70	847.26	146.61
-78.90	108.88	209.54	846.95	146.61
-79.01	108.60	210.77	846.49	146.60
-79.09	108.42	211.59	846.18	146.60
-79.21	108.16	212.80	845.74	146.60
-79.29	107.98	213.60	845.44	146.60
-79.40	107.71	214.80	845.01	146.60
-79.52	107.45	215.98	844.58	146.59
-79.59	107.27	216.76	844.30	146.59
-79.70	107.01	217.92	843.89	146.59

RC-4601 Condenser Duty (kW)	HC-Vapor Temp. (°C)	Heavy Oil Mass Flow (kg/hr)	Heavy Oil Density (kg/m^3)	Heavy Oil Flash Point (°C)
-79.82	106.75	219.07	843.48	146.58
-79.89	106.58	219.84	843.21	146.58
-80.00	106.32	220.97	842.81	146.58
-80.11	106.06	222.09	842.42	146.58
-80.22	105.81	223.20	842.03	146.57
-80.29	105.64	223.93	841.78	146.57
-80.40	105.39	225.03	841.40	146.57
-80.51	105.14	226.11	841.03	146.57
-80.61	104.89	227.18	840.66	146.57
-80.72	104.64	228.25	840.30	146.56
-80.82	104.40	229.30	839.95	146.56
-80.92	104.16	230.35	839.60	146.56
-80.99	104.00	231.04	839.37	146.56
-81.10	103.75	232.06	839.02	146.55
-81.20	103.52	233.08	838.69	146.55
-81.30	103.28	234.09	838.35	146.55
-81.40	103.04	235.10	838.02	146.55
-81.50	102.81	236.09	837.70	146.54
-81.59	102.57	237.07	837.38	146.54
-81.66	102.42	237.73	837.17	146.54
-81.72	102.27	238.37	836.96	146.54

RC-4601 Condenser Duty (kW)	HC-Vapor Temp. (°C)	Heavy Oil Mass Flow (kg/hr)	Heavy Oil Density (kg/m^3)	Heavy Oil Flash Point (°C)
-81.82	102.04	239.34	836.64	146.54
-81.92	101.81	240.30	836.34	146.53
-82.01	101.58	241.25	836.03	146.53
-82.11	101.36	242.19	835.73	146.53
-82.20	101.13	243.12	835.44	146.53
-82.30	100.91	244.05	835.14	146.53
-82.42	100.62	245.28	834.76	146.52
-82.51	100.40	246.19	834.47	146.52
-82.60	100.18	247.09	834.19	146.52
-82.72	99.89	248.28	833.82	146.52
-82.81	99.67	249.17	833.55	146.51
-82.90	99.46	250.05	833.28	146.51
-82.99	99.25	250.92	833.01	146.51
-83.11	98.96	252.08	832.66	146.51
-83.22	98.68	253.22	832.31	146.50
-83.31	98.48	254.07	832.05	146.50
-83.40	98.27	254.92	831.80	146.50
-83.48	98.06	255.76	831.55	146.50

B.2: Effect of RC-4602 condenser duty on various parameters

RC-4602 Condenser Duty (kW)	NC-Gases Temp. (°C)	Light Oil Mass Flow (kg/hr)	Light Oil Density (kg/m^3)	Light Oil Flash Point (°C)
-4.44	93.80	41.28	768.20	21.05
-4.99	92.59	46.37	768.13	20.99
-5.51	91.38	51.23	768.07	20.92
-6.00	90.20	55.88	768.00	20.85
-6.48	89.02	60.34	767.93	20.77
-7.08	87.48	66.00	767.82	20.67
-7.51	86.34	70.06	767.73	20.59
-8.06	84.83	75.22	767.59	20.50
-8.95	82.22	83.66	767.32	20.34
-9.54	80.38	89.27	767.12	20.23
-9.99	78.92	93.52	766.97	20.13
-10.52	77.11	98.58	766.80	20.00
-11.02	75.32	103.37	766.62	19.86
-11.50	73.54	107.92	766.45	19.72
-12.03	71.41	113.10	766.22	19.40
-12.54	69.29	118.00	765.98	18.89
-13.02	67.15	122.64	765.70	18.37
-13.55	64.64	127.77	765.34	17.75
-14.05	62.08	132.62	764.94	17.15
-14.53	59.46	137.20	764.50	16.67

RC-4602 Condenser Duty (kW)	NC-Gases Temp. (°C)	Light Oil Mass Flow (kg/hr)	Light Oil Density (kg/m^3)	Light Oil Flash Point (°C)
-14.98	56.77	141.53	764.05	16.44
-15.54	53.15	146.77	763.43	16.12
-16.01	49.79	151.13	762.87	15.81
-16.52	45.80	155.71	762.23	15.43
-17.01	41.57	159.96	761.59	15.02
-17.49	37.08	163.87	760.95	14.59
-18.04	31.22	168.20	760.16	14.11
-18.55	25.20	171.91	759.36	13.67
-19.04	18.73	175.25	758.49	13.13
-19.50	11.99	178.14	757.60	12.49
-19.99	3.92	180.96	756.61	11.66
-20.21	0.35	182.07	756.17	11.27

A:3: The Column Optimization Data

Condenser Duty kW			Mass Flow Rate (kg/hr)			Light oil/ Heavy oil Ratio	Density (kg/m^3)		Flash Point (°C)	
RC-4601	RC-4602	Total Duty	Light Oil	Heavy Oil	Total Oil		Light Oil	Heavy Oil	Light Oil	Heavy Oil
-78.16	-23.85	-102.02	217.82	201.85	419.67	1.08	759.90	849.89	12.85	146.63
-78.21	-23.84	-102.04	217.53	202.29	419.82	1.08	759.80	849.72	12.79	146.62
-78.29	-23.75	-102.04	216.67	203.16	419.83	1.07	759.72	849.37	12.75	146.62
-78.37	-23.67	-102.04	215.82	204.03	419.85	1.06	759.63	849.04	12.72	146.62
-78.45	-23.54	-101.99	214.74	204.90	419.64	1.05	759.63	848.71	12.75	146.62
-78.53	-23.45	-101.99	213.90	205.75	419.65	1.04	759.55	848.38	12.72	146.62
-78.62	-23.37	-101.98	213.06	206.60	419.67	1.03	759.46	848.05	12.69	146.61
-78.70	-23.28	-101.98	212.23	207.45	419.68	1.02	759.38	847.73	12.65	146.61
-78.78	-23.20	-101.98	211.40	208.29	419.69	1.01	759.30	847.41	12.62	146.61
-79.01	-21.64	-100.65	201.26	210.77	412.03	0.95	761.44	846.49	14.22	146.60
-80.00	-20.14	-100.14	187.83	220.97	408.80	0.85	761.27	842.81	14.35	146.58

Condenser Duty kW			Mass Flow Rate (kg/hr)			Light oil/ Heavy oil Ratio	Density (kg/m^3)		Flash Point (°C)	
RC-4601	RC-4602	Total Duty	Light Oil	Heavy Oil	Total Oil		Light Oil	Heavy Oil	Light Oil	Heavy Oil
-80.99	-19.12	-100.11	177.77	231.04	408.80	0.77	760.26	839.37	14.00	146.56
-81.66	-18.55	-100.21	171.91	237.73	409.63	0.72	759.36	837.17	13.67	146.54